https://doi.org/10.5194/essd-2024-236
Preprint. Discussion started: 30 October 2024

Open Access Earth System Science Data Discussions

POPE: a Global Gridded Emission Inventory for PFAS 1950-2020

Pascal Simon[1], Martin Otto Paul Ramacher[1], Stefan Hagemann[1], Volker Matthias[1], Hanna Joerss[1], and Johannes Bieser[1]

[1]Institute of Coastal Research, Helmholtz-Centre Hereon, Max-Planck-Straße 1, Geesthacht, 21502, Germany

Correspondence: Pascal Simon (pascal.simon@hereon.de)

Abstract. This study presents a global multi compartment Persistent Organic Pollutant Emissions model and inventory: POPE. The model computes temporally and spatially resolved model ready emissions for 23 of the most widely used Per- and Polyfluoroalkyl Substances (PFAS) distinguishing between emissions to air and emissions to water covering the time span from the first industrial scale production in 1950 up until 2020 on an annual basis on a grid with 0.5° resolution.

The POPE model distributes estimated total PFAS emissions in space and time based on several data sets such as the E-PRTR, NACE and US-EPA FRS in combination with socio-economic data as population and GDP complemented by estimates for individual point sources, such as industrial sites and airports, whereby the source activity is dependent on regional changes in production volumes, usage quotas, and recapturing efficiency over time. It includes emissions by industrial production, diffuse emissions through usage and disposal of consumer products, secondary emissions from the reaction of precursors, and emissions by firefighting exercises on airports using Aqueous Film Forming Foams.

It is demonstrated that the POPE emission inventory is compatible with current global emission estimates, and temporal and spatial variability of the emissions is explored. A comparison of independent measurements with modelled river concentrations based on the POPE emission inventory is provided. The POPE emission inventory is meant to be used as input for atmospheric and marine chemistry transport models, eventually allowing to assess the environmental fate of PFAS. POPE can be used to create hypothetical future emission scenarios, enabling model based predictions which can inform policy decisions. This is important given that even with a theoretical global fade-out of PFAS production, significant legacy pollution is still to be expected.

1 Introduction

Per- and Polyfluorinated Alkyl Substances (PFAS) constitute a group of substances known for their toxicity (Post et al., 2012)(Vierke et al., 2012), high persistence (Guelfo et al., 2021)(Cousins et al., 2020), and bioaccumulative nature within the food chain (Conder et al., 2008)(Martin et al., 2003). This characteristic leads to long-term exposure of human populations, raising significant concerns for both human health and the environment (Buck et al., 2011). Despite their known adverse effects, PFAS are widely used due to their stability, finding applications in water and dirt repellent coatings, food-packaging, outdoor apparel, furniture, firefighting foams, aerosol propellants, and heat transfer fluids. (Glüge et al., 2020)(OECD, 2004) However,

https://doi.org/10.5194/essd-2024-236
Preprint. Discussion started: 30 October 2024

this very stability contributes to their high risk for humans and the environment (Kirk et al., 2018). National and international effort has been made to regulate PFAS (Brennan et al., 2021b)(UNEP, 2020)(EC, 2022) but is constrained by competing interests and limited understanding. Therefore, understanding the behavior, fate, and effects of PFAS in the environment is crucial for mitigating their potential harm to human health and the ecosystem.

In addition to environmental measurements (Kannan et al., 2002)(Mclachlan et al., 2007)(Cousins et al., 2011)(De Silva et al., 2021), numerous numerical transport modeling studies of PFAS have been conducted to investigate and comprehend the fate of PFAS. These studies encompass global analyses, such as those conducted by by Stemmler and Lammel (Stemmler and Lammel, 2010), Armitage et al. (Armitage et al., 2006), and Thackray et al. (Thackray and Selin, 2017). Some studies focus on specific regions like Yarwood et al. (Yarwood et al., 2007) or water bodies like the Danube, as demonstrated by Lindim et al. (Lindim et al., 2015b), while others concentrate on specific PFAS emitters, as exemplified by Shin et al. (Shin et al., 2011).

A critical initial step in any transport modeling study is a temporally and spatially resolved emission inventory. However, for many PFAS, such data is either unavailable or lacks adequate attribution, resolution or spatiotemporal coverage. Several widely used estimates of global emissions for groups of PFAS, such as Perfluoroalkyl carboxylic acids (PFCAs), have been proposed by Wang et al. (Wang et al., 2014a), Prevedouros et al. (Prevedouros et al., 2006), and Armitage et al. (Armitage et al., 2009). Nevertheless, these global estimates are not spatially resolved. To tackle this problem, numerical modeling studies distribute PFAS emissions based on various spatial proxies, such as NO_x emission maps (Thackray and Selin, 2017). However, many of these modeling attempts do not allow for differentiation between emission sources, precursor reactions, or emissions to different environmental compartments. This differentiation, especially between emissions to the atmosphere and surface waters, is crucial for global long-range transport and multi-compartment modelling (Bieser and Ramacher, 2021) (Holland et al., 2020).

Motivated by this gap in current research, the present study introduces the Persistent Organic Pollutant Emission model (POPE) and its associated emission inventory. POPE aims to refine existing inventories to provide a global, consistent, scenario-capable (Matthias et al., 2018) emission model for PFAS emissions. The POPE model distinguishes between emissions released to water and emissions released to air, using a half-degree resolution grid and a temporal resolution of one year, spanning the years 1950 until 2020.

Building upon the extensive research conducted on widely used PFAS, such as PFOA and PFOS, POPE extends the knowledge and methods used to distribute these compounds in space and time to other PFAS for which data is more limited. This includes other PFAS from the groups of PFCAs and PFSAs, as well as precoursors that react under environmental conditions to form PFAS. Additionally, novel compounds, such as HFPO-DA and Adona, used as replacement for outlawed legacy compounds, are considered. POPE distributes known global inventories using proxies and socioeconomic data supported by field measurements, while also incorporating point sources such as airports and industrial sites.

The employed methodology begins with a discussion of global total emissions based on available data. This is followed by a description of the spatial disaggregation and temporal inter- and extrapolation applied in the POPE model. Each section is

https://doi.org/10.5194/essd-2024-236
Preprint. Discussion started: 30 October 2024

further divided based on emission sectors. Looking at the resulting POPE emission inventory, the consistency of POPE's global total PFAS emissions with other works is assessed. The subsequent chapter presents the spatial distribution of the POPE emission inventory and its global trends. Afterwards, the POPE emission inventory is evaluated using the Hydrological Discharge (HD) model (Hagemann et al., 2020) and several studies on PFAS river concentrations. Finally, the resulting POPE emission inventory is discussed with regard to its performance and data gaps.

2 POPE Inventory Construction

2.1 Modeled PFAS species

The POPE (Persistent Organic Pollutant Emission) inventory provides global gridded emissions for 23 individual Per- and Polyfluorinated Alkyl Substances (PFAS). POPE covers emissions to air and water for the time span 1950-2020. The 23 PFAS (table 1) considered in POPE are:

- 11 Perfluoroalkyl carboxylic acids (PFCAs)
- 4 Perfluorosulfonic acids (PFSAs)
- 5 Fluorotelomer alcohols (FTOHs)
- Perfluorooctanesulfonamide (FOSA)
- 2 replacement compounds (HFPO-DA and Adona)

The chosen species are those currently regulated under Annex A and B of the Stockholm Convention (UNEP, 2020) and those about to be regulated by the European Commission (EC, 2022) excluding the replacement compound "C6O4" due to the limit of available data. Additionally, novel replacement compounds hexafluoropropylene oxide dimer acid (HFPO-DA, also known under the brand name Gen-X) and ammonium 4,8-dioxa-3H-perfluorononanoate (known under the brand name Adona) were included due to their anticipated future importance (Joerss, 2020)(Munoz et al., 2019). A detailed list of all included compounds is given in table 1

https://doi.org/10.5194/essd-2024-236
Preprint. Discussion started: 30 October 2024

Table 1. PFAS included in the POPE emission inventory.

Group	Carbon-Moieties	Short Name	Long Name
PFCAs	4	PFBA	Perfluorobutanoic Acid
	5	PFPeA	Perfluoropentanoic Acid
	6	PFHxA	Perfluorohexanoic Acid
	7	PFHpA	Perfluoroheptanoic Acid
	8	PFOA	Perfluorooctanoic Acid
	9	PFNA	Perfluorononanoic Acid
	10	PFDA	Perfluorodecanoic Acid
	11	PFUnA	Perfluoroundecanoic Acid
	12	PFDoA	Perfluorododecanoic Acid
	13	PFTrA	Perfluorotridecanoic Acid
	14	PFTeA	Perfluorotetradecanoic Acid
PFSAs	4	PFBA	Perfluorobutanesulfonic Acid
	6	PFHxS	Perfluorohexanesulfonic Acid
	8	PFOS	Perfluorooctanesulfonic Acid
	10	PFDS	Perfluorodecanesulfonic Acid
FTOHs	4 + 2	4:2 FTOH	4:2 Fluorotelomer Alcohol
	6 + 2	6:2 FTOH	6:2 Fluorotelomer Alcohol
	8 + 2	8:2 FTOH	8:2 Fluorotelomer Alcohol
	10 + 2	10:2 FTOH	10:2 Fluorotelomer Alcohol
PFECAs	6	HFPO-DA	Hexafluoropropylene Oxide Dimer Acid
	7	Adona	Ammonium 4,8-Dioxa-3H-Perfluorononanoate
	8	FOSA	Perfluorooctanesulfonamide

2.2 Emission and proxy datasets used by POPE

POPE uses several available datasets for direct and indirect emission estimation. These include aggregated emission estimates based on the total global emission inventories of Wang (Wang et al., 2014a), Prevedouros (Prevedouros et al., 2006), and Armitage (Armitage et al., 2009). Additionally several data sets of known point sources or regional datasets as well as aggregated emissions for regional compartments are included.

POPE temporally and spatially downscales the aggregated PFAS emissions into a global 0.5x0.5° gridded annual emission dataset suitable for chemistry transport models (CTMs). The downscaling is based on publicly available socioeconomic data sets. Besides this, time series of environmental observations of PFAS are used to estimate levels and trends in source activity.

POPE uses:

https://doi.org/10.5194/essd-2024-236
Preprint. Discussion started: 30 October 2024

- Global emission datasets
  - Global emission inventory for PFCAs 1951-2004 by Prevedouros et al.(Prevedouros et al., 2006)
  - Extension of the emission inventory by Prevedouros et al. with estimations considering distribution across large spatial scales and environmental compartments by Armitage et al.(Armitage et al., 2009)
  - Global emission inventory for PFCAs (C4-C14) 1951-2030 partly building on Prevedouros et al. by Wang et al.(Wang et al., 2014a)(Wang et al., 2014b)
- Point source emission registers
  - European pollutant release and transfer register (E-PRTR) containing locations of relevant industries in Europe, 2007-2020(EC, 2023)
  - Nomenclature statistique des activités économiques (NACE) Rev. 2 providing sub-national data on number of sites and of employees for relevant industries in Europe, 2008 (Nace)
  - Facility Registry Service (FRS) of the United States Environmental Protection Agency providing relevant locations in the United States, 2020(EPA, 2023)
- Individual emission data for large point sources
  - Purchasing records, production volumes and estimated losses for the Dupont Plant Parkersburg West Virginia by Paustenbach et al.(Paustenbach et al., 2007a)
  - Multiple fluoropolymer production sites globally (Will, 2005)(Wang et al., 2014a) (Prevedouros et al., 2006)
  - Production volumes and used PFAS for several plants in Europe (Dalmijn et al., 2023)
  - Swedish airports (Ahrens, 2009)(Filipovic et al., 2013b)
- Local emission data
  - Large Emitters in Sweden(OECD Environment Directorate, 2018)
  - Emitters in the Danube watershed (ICPDR, 2003)
  - Emission load in a boreal watershed(Filipovic et al., 2015)
  - Emissions in European rivers in 2008(Loos et al., 2009)
  - Emissions to the Baltic Sea(Filipovic et al.)
  - Emissions caused by US WWTPS (Hamid and Li, 2016)

Furthermore POPE uses multiple datasets for the distribution and transport of known emissions, These are:

- Socio-economic datasets

https://doi.org/10.5194/essd-2024-236
Preprint. Discussion started: 30 October 2024

- Population density data 1950-2020 (Chambers, 2020)
- Georeferenced GDP data 1990-2015 (Kummu et al., 2018)
- Global dataset of airport designations 2020 (ICAO, 2014)
- US WWTP runoff 1930-2000 (Hale et al., 2015)

- Environmental datasets
  - Global Soil Wetness Project Phase 3 forcing data, 1950-1978 (Dirmeyer et al., 2006)
  - WATCH Forcing Data based on ERA5 re-analysis 1979-2020 (Cucchi et al., 2020)

2.3 Emission sectors

The produced emission dataset distinguishes emissions for each PFAS or precursor species (Table 1) for each of the 6 source sectors (Table 2). The industrial manufacturing sector dominates the total emissions for many PFAS. The single largest emitter of PFAS is fluoropolymer production which is estimated to account for over 70% of the total global perfluoroalkyl carboxylic acid (PFCA) emissions from 1951 to 2004 (Prevedouros et al., 2006). It is assumed to be the largest contributor to the global inventory of PFCAs and PFSAs (Cousins et al., 2011)(Lim et al., 2011) pre 2001 and might be the largest source for their replacements like PFECAs and FOSA in the future (Wang et al., 2013)(Scheringer et al., 2014). Apart from fluropolymer production, other industries like textile manufacturing, coating of surfaces or electronics are important industrial emission sources. As a smaller but locally very significant source, Aqueous Film Forming Foams (AFFF) used for airport firefighting and firefighting excercises is also taken into account.

POPE employs different methods for the emission estimation of each individual sector. Table 2 gives an overview of the used methods and the data sources for each sector.

In the following sections, we will describe the individual sectors in detail and explain how annual total emissions were estimated for each of them.

As a general approach POPE estimates annual total emissions of a compound for a given single industrial point-source or region. Production emissions are estimated based on production volumes, which are modulated by changing activity rates, loss fractions, and compartmental coefficients where applicable as discussed in section 2.3.1. Where the data for this bottom-up approach is not sufficient, available regional emission estimates are distributed. For the US and Europe that is mostly based on known registered sites with respect to their number of employees, if available, as shown in section 2.3.2. For most other countries diffuse emissions are distributed by population and GDP as a proxy illustrated in section 2.3.3. The same applies for product use and dispoal unless data on Waste-Water-Treatment-Plants (WWTPs) or landfills are available. AFFF emissions are estimated by airport size and designation shown in detail in section 2.3.4.

https://doi.org/10.5194/essd-2024-236
Preprint. Discussion started: 30 October 2024

Open Access Earth System Science Data Discussions

Table 2. Overview of the sectors in POPE with the employed methods and data sources to obtain the respective emission estimations.

Sector	Method	Sources
Fluoropolymer production	Bottom-Up, based on extrapolated production quantities, losses modeled after Parkersburg WV plant	(Wang et al., 2014a) (Paustenbach et al., 2007a) (Prevedouros et al., 2006)(Will, 2005)(Dalmijn et al., 2023)
Other Industries	Top-Down, known totals distributed by countrygroup, individual sites (E-PRTR, US-EPA FRS), emissions scaled by number of employees where applicable	(Wang et al., 2014a)(Glüge et al., 2020)(Prevedouros et al., 2006)
Product Use	Mixed Top-Down and Bottom-Up, emissions per capita based on measurements in Europe, adjusted per country group, scaled with GDP	(Loos et al., 2009)(Lindim et al., 2015a) (Chambers, 2020)(Kummu et al., 2018)
Disposal	Top-Down, known totals distributed by countrygroup, individual sites (E-PRTR, US-EPA FRS), WWTPs scaled by outflow	(Hale et al., 2015)(EPA, 2023)(EC, 2023)
AFFF	Bottom-Up, based on exemplary airports in Sweden, applied to airport dataset, emissions scaled by airport size	(Ahrens, 2009)(Filipovic et al., 2013a)(OECD Environment Directorate, 2018)

2.3.1 Fluropolymerproduction

Fluoropolymer production is the most important source for many PFAS and thus receives special attention in POPE. The process is based on the most extensively researched fluropolymer production plant of the company Dupont in Parkersburg, West Virginia and the extensive data published by Paustenbach et al. (Paustenbach et al., 2007a). This data helps to relate available fluoropolymer production volume V found for different plants in economic datasets to actual emissions of PFAS. This is done with two additional factors: a usage rate and a loss fraction. The usage rates c describes how much of the corresponding PFAS is needed per ton of produced Fluoropolymer V. The loss fraction f describes how much of the used PFAS is expected to be lost in the process and to which environmental compartment (air or water) it is emitted.
Building on this, the expected PFAS emission E[kg] is calculated depending on the medium as

$$E_{medium} = V \cdot c \cdot f_{medium}, \tag{1}$$

with the production volume V[kg], loss-fraction f[-] to the corresponding compartment and the usage rate c[-]. With respect to fluoropolymer production, the individual production volumes of sites are based on multiple sources. Several approximated production volumes for different years are taken from Wang et al.(Wang et al., 2014a), Paustenbach et al. (Paustenbach et al., 2007a) Will et al.(Will, 2005) and Dalmijn et al.(Dalmijn et al., 2023). This allows POPE to consider the production of Polytetrafluoroethylene (PTFE), fluorinated ethylene propylene (FEP), Polyvinylidene fluoride (PVDF), and perfluoroalkoxy alkane (PFA) as point sources. As PFAS are typically not the monomers itself but rather polymerization aids, the applied loss

https://doi.org/10.5194/essd-2024-236
Preprint. Discussion started: 30 October 2024

fraction and usage rate are specific to the PFAS used in the production process and the produced fluropolymer. Ususally both are not fixed and depend on the process used, which is not necessarily publicly known for each plant. Wang et al. (Wang et al., 2014a), Paustenbach et al. (Paustenbach et al., 2007b) and Prevedouros et al. (Prevedouros et al., 2006) provide ranges for the usage rate which POPE takes into account for the upper and lower bound emission scenarios.

For the loss fractions different measurements are available (Wang et al., 2014a), with the most extensive study published by Paustenbach et. al. (Paustenbach et al., 2007a) based on purchasing records. Differences in estimated loss fractions are again used to define higher and lower bound estimates.

2.3.2 Other industries

Smaller fluoropolymer production plants and other industries are also considered in POPE. Unlike the bigger plants, these are disaggregated via a top down approach. Based on production and emission estimates, PFAS emissions are disaggregated for the following industrial sectors:

- Apparel manufacturing
- Aerospace product and parts manufacturing
- Manufacturing of chemicals and chemical products
- Manufacturing of computer, electronic and optical products
- Semiconductor and other electronic component manufacturing
- Treatment of fibres or textiles
- Manufacturing of furniture
- Motor vehicle and parts manufacturing
- Paint, coating, and adhesive manufacturing
- Manufacturing of paper and paper products
- Resin, synthetic rubber, and artificial and synthetic fibers and filaments Manufacturing
- Manufacturing of rubber and plastic products
- Surface treatment of metals and plastics
- Manufacturing of textiles

https://doi.org/10.5194/essd-2024-236
Preprint. Discussion started: 30 October 2024

Each sector is of varying importance, specific for each compound.

The contribution of each sector to the total emissions is based on the estimations by Wang et al. (Wang et al., 2014a) and Prevedouros et al. (Prevedouros et al., 2006). As HFPO-DA and Adona are mainly used as direct replacements (Joerss, 2020)(Munoz et al., 2019), their totals are related to the substituted volume of processing aid.

This is done by using fixed replacement factors based on Dalmijin et al. (Dalmijn et al., 2023), Gebbink et al. (Gebbink and van Leeuwen, 2020), Brandsma et al. (Brandsma et al., 2019) and Zarebska et al. (Zarębska et al., 2024) feeding into the upper and lower bound estimates with the arithmetic mean used as the best guess estimate. It is assumed that the production of related facilities does not change over the switch and carries on with identical growth factors and loss fractions and with complete substitution with the appropriate replacement. This corresponds to multiplication of the emissions by the replacement factors. The appropriate replacement is chosen based on the associated company. GenX is produced by Dupont, whereas Adona is a 3M/Dyneon product. Both can be used as a replacement for PFOA in PTFE production or PFNA in PVDF production respectively.

FOSA is handled differently to all other compounds as no global totals and no production data is available. The total emission is approximated by using measured concentrations and their relation to PFOS as a proxy. This is due to FOSA being a precoursor to PFOS and their uses being very closely related (Pickard et al., 2022). For this purpose water samples and samples in biota are available (Soerensen and Fraxneld, 2023 (Soerensen and Faxneld, 2023); Pickard et al., 2022(Pickard et al., 2022)). The ratios in biota are corrected by dividing them by the bioaccumulation factors calculated by Soerensen and Faxneld (Soerensen and Faxneld, 2023). All measurements are averaged over the respective regions. This gives estimated total FOSA emissions of 2.5% and 1.1% of PFOS emissions in Europe and the United States respectively.

2.3.3 Product Use and Disposal

The second largest contributor to total emissions of PFAS is the release by PFAS containing products during their life cycle(Pistocchi and Loos, 2009)(Glüge et al., 2020). The range of such products, from outdoor jackets and furniture to floor wax and dental floss, is very broad and there is only limited data available on the total usage of these products, their PFAS content, and the associated PFAS loss over time.

The total emissions during lifetime of PFAS containig products in a given area is related to the population of that area (top-down), which in turn gives an estimate of the emissions by product use of one individual. This is eventually used for the local emissions of other areas (bottom-up). Assuming sufficient locality and only slow changes over time, this can be achieved with the total emission load of rivers and the population in their watershed. Similar approaches have been used before, for example

https://doi.org/10.5194/essd-2024-236
Preprint. Discussion started: 30 October 2024

by Lindim et al. (Lindim et al., 2015a). The relation of the river emission load to a corresponding atmospheric load has to be assessed in a second step afterwards.

The total load of a river is calculated by the river runoff and a reliable PFAS concentration measurement at the estuary. This has for example been done for PFOA and PFOS by Pistocchi and Loos (Pistocchi and Loos, 2009) as well as Mclachlan et al. (Mclachlan et al., 2007) for major European rivers. Rivers with known major contributors such as PTFE production sites are ruled out, so that the emissions caused by these are not taken into account twice. Performing a linear and a log-linear regression between population in the watershed and annual PFOA load leads to a PFOA Emission $E[\mu\text{g/day}]$, depending on the population p according to

$$E = 19.2 \frac{\mu\text{g}}{\text{person} \cdot \text{day}} \cdot p \tag{2}$$

for a linear regression and

$$E = 5.1 \frac{\mu\text{g}}{\text{person} \cdot \text{day}} \cdot 10^{-4} \cdot p^{1.2841} \tag{3}$$

for a log-linear regression. Performing the same for PFOS Emissions $E[\mu\text{g/person/day}]$ yields

$$E = 6.4 \frac{\mu\text{g}}{\text{person} \cdot \text{day}} \cdot p \tag{4}$$

for a linear regression and

$$E = 3.5 \frac{\mu\text{g}}{\text{person} \cdot \text{day}} \cdot 10^{-4} \cdot p^{1.0115} \tag{5}$$

The linear regression suggests lower emission values than the exponential regression, therefore POPE uses the linear regression for the lower bound, whereas the log-linear regression is used for the upper bound. As this data is not available for other compounds than PFOA and PFOS, it is assumed that the product use of PFCAs and their replacements scale similarily with poulation as PFOA, whereas PFSAs and their replacement follow the trend of PFOS. In both cases the prescribed total is conserved.

2.3.4 Aqueous Film Forming Foams

Aqueous Film Forming Foams are relevant for firefighting training and operational use on airports. As airport emissions play a minor role in the total inventory, they are typically considered for global emissions but not spatially resolved. On a regional/local scale on the other hand, airport firefighting emissions might still dominate PFAS emissions (Ahrens et al., 2015). This is mainly due to the fact, that especially in remote regions and low population density areas air transportation of passengers and goods becomes relatively more important, as it is for example the case in Sweden (Hansson et al., 2016).

https://doi.org/10.5194/essd-2024-236
Preprint. Discussion started: 30 October 2024

The POPE model focuses on bottom-up emission estimations of individual airports. The 60 biggest airports worldwide are handled individually while all other relevant airports are categorized in 5 categories where each category gets assigned a single emission load.

Available Data regarding the PFAS emissions of airports includes measurements at Arlanda Airport, Stockholm, Sweden by Ahrens et al. (Ahrens et al., 2015), measurements near a military airport near Stockholm by Filipovic et al. (Filipovic et al., 2015), and the estimated total PFOA emission of airports in Sweden, based on the PFAS-content and their total use of PFAS-based firefighting foam (Hansson et al., 2016).

The regulations of the International Civil Aviation Organization (ICAO) requires the number of fire-departments, firefighting trucks or firefighters to scale among other factors with the number of flights an airport receives (ICAO, 2014). Therefore the amount of firefighting foam used, and with that, the volume of PFAS emitted, is assumed to scale with the number of firefighters employed using AFFF for their regular exercises. Thus, the PFAS emission of the 60 biggest airports worldwide is scaled in relation to the number of flights per year, relative to Arlanda Airport.

Data on the yearly number of flights is not available for every airport worldwide. For the estimation of emissions of smaller airports, this work makes use of the locations of airports according to the IATA and ICAO Databases (ICAO, 2014) and the report by the Nordic Council of Ministers (Goldenman et al., 2019). The ICAO dataset categorizes airports in 3 different size classes. All relevant classes cover about 6500 airports. Airports are differentiated as of primarily civilian or primarily military use by designation, since there is a huge disparity in emissions (Linderoth et al., 2016). All small civilian airports are dropped due to their insignificance, leaving estimates for medium civilian, small military and medium military airports to be considered.

Following Ahrens et al. (Ahrens et al., 2015) the medium civilian airport emissions are obtained by subtracting the emissions of Arlanda Airport from the total PFAS emissions attributed to civilian airports in Sweden as estimated by Hansson et al. (Hansson et al., 2016) and dividing the remainder by the number of medium airports. The same approach is taken for the military airports based on Filipovic et al. (Filipovic et al., 2015), where three size classes add an additional degree of freedom. It is assumed, that the fraction of emissions between medium and small military airports is the same as between medium and large military airports. This leads to the approximated emission factors per airport shown in table 3

This allows each individual airport to be assigned an emission based on its size and usage.

https://doi.org/10.5194/essd-2024-236
Preprint. Discussion started: 30 October 2024

Table 3. Emission factors per airport relative to Stockholm Arlanda Airport based on (Ahrens et al., 2015) and (Filipovic et al., 2015).

emission factor [-]	small	medium	large
civilian	0	0.6	1.0
military	0.4	1.0	2.6

2.4 Spatial disaggregation

290 POPE accounts for emissions as point sources where an approximation of the emitted volume of PFAS at a specific location is available. Point sources include the major fluoropolymer production facilities, major other industrial sources, AFFF emissions from airports, and major waste disposal sites.

The remaining emissions are then spatially disaggregated as area sources with a half-degree grid resolution, whereby the 295 disaggregation method depends on source sector and region. Following Wang et al. (Wang et al., 2014a), countries are divided into three groups. Depending on the group different methods and spatial proxies for area emission disaggregation are applied.

- Group I: Early adopters of PFAS related industries
  Western Europe, North America and Japan
- Group II: Current focus of PFAS related industries
300 China, India and Russia
- Group III: Consumers of PFAS products
  Rest of the world, including the complete southern hemisphere.

2.4.1 Point sources

2.4.2 Fluropolymerproduction and other industries

305 The majority of industrial sources in Country Group I such as the historically very important sites in Europe, Japan and the United States are implemented as point sources. Moreover, the most important fluoropolymer production sites in country Group II, primarily located in China, can be modelled as individual point sources. All other industrial emissions are distributed as area sources based on socio-economic data which will be discussed in section 2.4.4.
The locations of industries and manufacturing sites in POPE are a collection of several data sets of individual sources as shown 310 in section 2.3.1. Because of their importance POPE considers 26 fluoropolymer production sites individually. Depending on the time frame, these correspond to up to 90% of the total fluoropolymer production (Wang et al., 2014a). These production sites are situated in Europe, the USA, and Japan with newer ones found in east Asia, mainly China.

https://doi.org/10.5194/essd-2024-236
Preprint. Discussion started: 30 October 2024

The emissions of all other industries are spatially distributed top-down based on their relative importance. For this, several datasets are available. In Europe POPE makes use of the European Pollutant Release and Transfer Register (E-PRTR) (EC, 2023) and the statistique des activités économiques dans la Communauté européenne (NACE) Rev. 2 (Nace). For the United States POPE includes the Facility Registry Service (FRS) by the United States Environmental Protection Agency (EPA, 2023). The E-PRTR contains 60 000 sites from 65 economic activities. Based on the usage of PFAS as reported by Wang et al. (Wang et al., 2014b), Prevedouros et al. (Prevedouros et al., 2006) Brennan et al. (Brennan et al., 2021a), and the corresponding OECD Report(OECD, 2004)(OECD, 2006)(OECD, 2011)(OECD Environment Directorate, 2018), 24 of them where deemed relevant for PFAS emissions.The E-PRTR sites are listed with precise coordinates but include no consistent data regarding their emissions or production volume.

The Nace Rev. 2 dataset (Nace) complements this, as it provides sector specific industry data based on the Nomenclature des unités territoriales statistiques (NUTS) levels. This data relates to wider regions rather than individual points but includes not only the number of relevant sites, but also size related data such as economic activity and number of employees.

POPE uses a two tracked approach incorporating the E-PRTR and NACE distributing half of the relevant emission fraction based on individual locations an the other half by the total number of employees, assuming a homogeneous distribution inside the corresponding NUTS region.

The FRS covers 95 individual sites in the United States categorised by sector, similar to the E-PRTR. Out of the 95 sectors, 15 were deemed relevant to the emission of the included PFAS based on the known usage of PFAS (Glüge et al., 2020). Building on the per country estimates by Wang et al. and Prevedouros et al., emissions are again distributed top-down equally between sites, based on the individual contribution of a given sector.

2.4.3 Product disposal

The spatial distribution of emissions by product disposal in country group I is handled similar to the industrial manufacturing as distribution on a per site basis. In country groups II and III the spatial distribution of disposal emissions is identical to the product use emissions.

Data on disposal sites is available for Europe via the E-PRTR (EC, 2023) and Nace Rev. 2(Nace) and for the United States via a dataset by Hale et al. (Hale et al., 2015) and the FRS(EPA, 2023). POPE distinguishes between waste water treatment plants, which emit exclusively to the water, waste incineration sites, which emit to the atmosphere, and landfills, where both compartments are important for transport (Hepburn et al., 2019)(Lang et al., 2017).

The Nace Rev. 2 and E-PRTR datasets contain individual categories for landfillls and waste water treatment plants and the

https://doi.org/10.5194/essd-2024-236
Preprint. Discussion started: 30 October 2024

emissions are distributed accordingly. Nace is again operating on a coarser spatial scale while providing the more extensive dataset, in contrast to the E-PRTR, which contains less sites but with the exact geographical location. Both are weighted equally for the emission distribution.

For the United States POPE includes the corresponding categories in the US EPA FRS as well as an extensive dataset on waste water treatment plants by Hale et al. (Hale et al., 2015). While the FRS only considers geographic locations, which are therefore treated identically, the dataset by Hale et al. contains outflows for each waste water treatment plant allowing to scale the emissions by the amount of processed waste water. Again, both datasets are weighted equally for emission distribution.

2.4.4 Area Sources

2.4.5 Fluoropolymer production and other industries

Area sources are used for the emission distribution for industrial sources for countries in Country Group I which are not yet taken into account, as well as smaller sites in Country Group II. Without further information on the distribution over the corresponding sites, emissions are distributed by population and GDP as a proxy for industrialisation (Bieser et al., 2011) (Matthias et al., 2018) (Kuenen et al., 2022). The population data set is published by J. Chambers (Chambers, 2020) and is available at half degree resolution providing yearly numbers. It combines datasets from ISIMIP Histsoc from 1950 to 1999 and the GPWv4 dataset from 2000 to 2020. The GDP data set of Kummu et al. (Kummu et al., 2018) is available for 1990 to 2015 at a resolution of 5 arc-minutes, but effectively accounts for annual GDP per capita on a state by state level. The GDP is adjusted for inflation and aggregated to the resolution of the population dataset.

The approximated total emissions of the sector E_{tot} are distributed over all corresponding grid cells according to their GDP ($GDP_{i,j}$) as a fraction of the total accumulated GDP ($\sum GDP_{i,j}$):

$$E_{i,j} = E_{\text{tot}} \cdot GDP_{i,j} \cdot \left(\sum GDP_{i,j} \right)^{-1}. \tag{6}$$

This process excludes the territory of the United states and the European Union as these are already taken into account as well as all countries assigned to Country Group III, due to their minimal PFAS production capacities.

2.4.6 Product use

The emissions caused by product use are diffuse sources, which are calculated on a per grid cell basis. The grid resolution of 0.5 x 0.5 degrees is based on the input data sets.

To spatially represent the product use related emissions, the datasets for the population and GDP are utilised, again. As the used river concentration data by Pistocchi et al. (Pistocchi and Loos, 2009) only considers European rivers, it is expected, that applying this data globally overestimates the product related emissions. Therefore, it is assumed that the use of PFAS-related

https://doi.org/10.5194/essd-2024-236
Preprint. Discussion started: 30 October 2024

products scales with GDP per capita. The mean GDP of the European Union for the year 2008, when the data of Pistocchi and Loos (Pistocchi and Loos, 2009) applies, is used as a baseline. This leads to an emission of PFAS per person and US Dollar economic performance.

Taking the introduced datasets and assumptions into account, the product related emissions of a grid cell $E_{i,j}$ are computed as

$$E_{i,j} = P_{i,j} \cdot \frac{GDP_{i,j}}{\overline{GDP}_{Europe}} \cdot f, \tag{7}$$

with the corresponding grid cell population $P_{i,j}$[inhabitants], the grid cells Gross-Domestic-Product $GDP_{i,j}$[$], the average Gross-Domestic-Product of the European Union $\overline{GDP}_{Europe}$[$] and the calculated per person emissions $f\left[\frac{\text{kg}}{\text{inhabitant}}\right]$.

2.5 Temporal Development

One of the main goals of this emission model is to cover the whole time span since the first production of PFAS until the present day, i.e. from 1950 to 2020 with a temporal resolution of one year. This chapter illustrates the variation of industrial emissions over time.

2.5.1 Fluoropolymer production

As the main sources are industrial sites, there is no expected seasonality in the grand total of emissions. The minimal seasonality of small emission contributors, for example the use and disposal of outdoor clothing, is assumed to be much smaller than industrial trends or seasonal variation due to environmental conditions.

Temporal changes in PFAS emissions from industrial production are primarily influenced by three factors. Firstly, the global increase in PFAS production volume, secondly, the impact of changes to capture and reprocessing technology on the loss fraction; and finally, changes in factory operations including, but not limited to, the impact of national and international regulations. In addition to the overall total, there are discernible regional variations that may align with or oppose the global pattern, thereby resulting in a spatial redistribution.

2.5.2 Changes in Production Volume

The main reason for temporal variability in the emission of a single site is changing production volume. Modeling the changes in production volume is challenging, as most companies do not publish exact site specific production volumes. Contrary to that, Paustenbach et al. (Paustenbach et al., 2007a) published the total amount of used APFO for PTFE production in the Dupont industrial site in Parkersburg West Virginia from 1951 to 2003 based on purchasing records. This is shown in figure 1. This dataset will be used as a basis for the model.

https://doi.org/10.5194/essd-2024-236
Preprint. Discussion started: 30 October 2024

Open Access Earth System Science Data Discussions

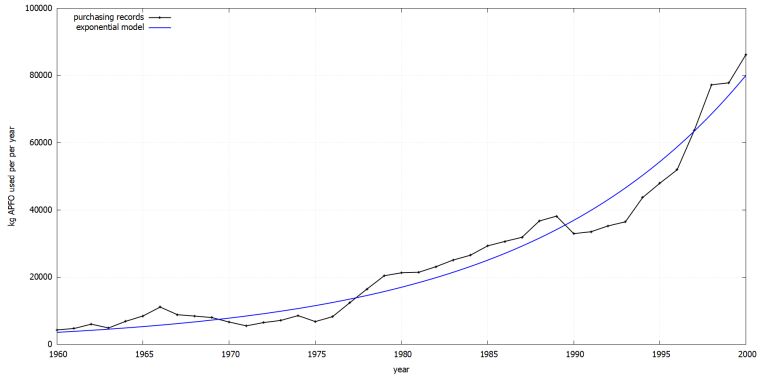

Figure 1. Total amount of APFO used in fluoropolymer production at the Dupont Parkersburg plant from 1951 to 2001 based on purchasing records. Adapted from Paustenbach et al. (Paustenbach et al., 2007a). The blue curve represents the exponential approximation used by POPE for fluoropolymer production plants in country group I.

Observable in the timeseries of used APFO in Parkersburg is the seemingly exponential increase up to the year 2000. As there is no known change in APFO usage rates this increase is attributed fully to an increase in production volume. An exponential fit to this part of the curve yields a yearly growth factor of 0.074 with $R^2 = 0.96$.

Based on this example it can be assumed that without regulation or fade out an exponential increase in fluoropolymer production volume is reasonable.

Consequently, an exponential fit of the yearly fluoropolymer production volume is used for the remaining 25 production sites. For 11 of these, several years with approximated production volumes were available so that individual growth factors could be calculated. For the remaining 14 production sites only the production volume of one year is known. In these cases the average growth factor of plants where more data is available within the region was averaged and applied. These growth factors can be found in table 4.

Table 4. Fluoropolymer production growth factors obtained through exponential regression for known production quantities in each country applied over the complete timespan.

Asia without Japan	Japan	North America & Europe
0.225	0.041	0.074

For all fluoropolymer production sites, the opening and closing of factories is considered, specifically closings due to country specific regulations and bans. The production volume before the opening of a factory and after closure is set to zero accordingly.

https://doi.org/10.5194/essd-2024-236
Preprint. Discussion started: 30 October 2024

This is a simplification as after closure of a production site significant residual emission is expected, but already accounted for beforehand. Depending on the used transport model and circumstances, a retardation of emissions may be needed.

This allows to obtain an approximate production volume V for all included sites over the covered timespan to calculate the emissions according to equation 8.

2.5.3 Loss Fraction

As a second source of temporal change, the loss fraction according to equation 1 is included. The changes in loss fraction were subject of the study of Wang et al. (Wang et al., 2014a). The authors differentiated between five periods with estimated loss fractions to water and air. Since the main concerns for these shifts were of economical nature, as for the early shifts the worrying effects on the environment were not yet known, it was assumed that country specific regulations played a minor role. Therefore no country specific scaling was performed here. The loss fractions were smoothed out over 10 years each to represent the expected gradual transition due to the adaptation of new technology. The temporal development of the loss fraction is depicted in figure 2

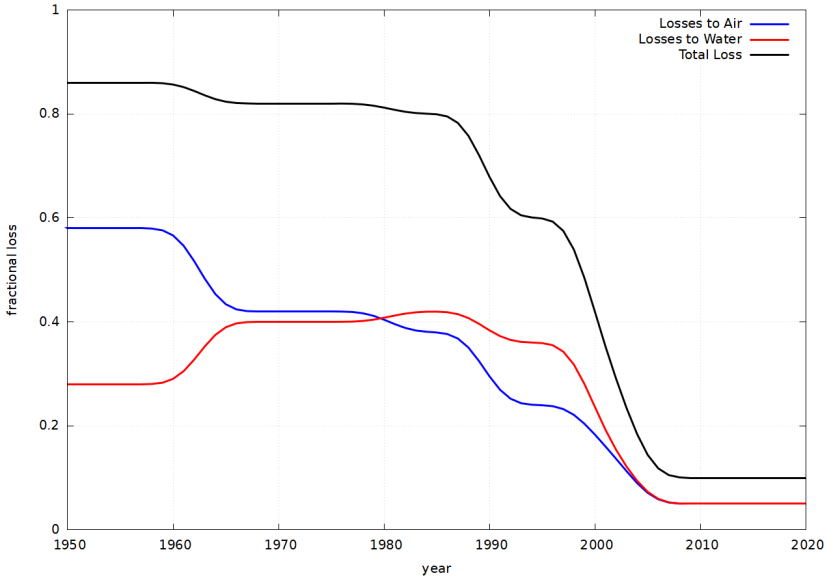

Figure 2. Loss fractions taken from (Wang et al., 2014a) smoothed out over a 10 year period.

The emissions in a specific scenario s into medium m at time t $E_{s,m,t}$ are therefore approximated by

$$E_{s,m,t} = V_{\text{ref}} \cdot \mathrm{e}^{k_s \cdot (t - t_{\text{ref}})} \cdot c_s \cdot f_{m,t}, \tag{8}$$

https://doi.org/10.5194/essd-2024-236
Preprint. Discussion started: 30 October 2024

with the growth factor k depending on the scenario s, the reference production V_{ref} in the reference year t_{ref} the usage rate c_s, depending on the scenario and the loss fraction $f_{m,t}$ at time t to the corresponding medium m .

2.5.4 Other industries

Ohter industries than fluoropolymer production are handled methodically different in POPE. In this case loss fraction and usage rates are not applicable as neither the produced product quantities, nor the used PFAS mass per product volume are known. The temporal dynamics of emissions is therefore solely determined by the total estimated production volume of a site, assessed according to chapter 2.3.2. The lower bound scenario assumes only linear growth forward in time from the corresponding reference period, as well as exponential growth backwards in time. The upper bound assumes exponential growth forward in time as well as linear growth backwards in time. The prescribed sector total is conserved in both cases.
Note that regarding the location of industrial sites no temporal change has been applied. The corresponding datasets (US EPA FRS, E-PRTR, and Nace Rev.2) are only available for recent years. It is therefore assumed that outside of fluoropolymer production no spatial shift of emissions over time apart from varying production growth rates and different regulatory impact takes place.

2.5.5 Product Use and Disposal

POPE assesses the temporal change in emissions due to product use and product disposal together. It is assumed that the emissions of waste water treatment plants and disposal sites follow the temporal trends of the related product emissions. As will be addressed, a time lag is implicitly included due to the nature of the included data. The actual time lag of disposal sites may be much larger than modeled by POPE.

The emissions of PFAS related products are changing over time via two different factors. On the one hand shift occurs implicitly with changes of population and GDP via their respective datasets. On the other hand, explicit scaling over time has to be applied to represent the growth in use of PFAS related products. Both factors will be explained subsequently.

As shown in the dataset by Chambers (Chambers, 2020) the population mostly follows exponential growth, although the growth factors are varying and are generally lower in country group I, and higher in country group II and III. Although the World's population approximately tripled from 1950 to 2020, the population in country group I grew on average about 50%. Regarding the GDP, Kummu et al. (Kummu et al., 2018) provided data from 1990 to 2015. The GDP before and after this time period is extrapolated assuming exponential growth, using the average annual growth over the provided period as annual growth factor. This results in a global real GDP growth which is approximately five fold, with the same distributional trends as the population. The PFAS emissions grow implicitly with population and GDP.

https://doi.org/10.5194/essd-2024-236
Preprint. Discussion started: 30 October 2024

Apart from more people having more income available for consuming PFAS containing products, the growing prevalence of PFAS products in the market has to be captured by POPE. As an approximation, it is assumed that the use of these products grows proportionally with the industrial production volumes. Even though not all industrial production is exclusively for the consumer market, this is a proxy for the prevalence of PFAS containing products and forces zero product related emissions, before their first production.
The estimated production volume of PFOA and PFOS in the year 2009, when the study by Pistocchi and Loos (Pistocchi and Loos, 2009) was performed, serves as a benchmark production for these compounds. The product use and disposal emissions of a year are scaled by the fraction that the corresponding year's production volume represents of the benchmark production volume. This also implicitly accounts for a part of the emission time lag. This scaling is performed crosswise for the higher and lower bounds of the production volume and the emission per person, respectively.

One additional influence that POPE considers is the conflation of both factors, as for example production increases because there is more economic power demanding PFAS containing products.
This conflation is considered for the upper and lower bounds. Since the majority of the data set is extrapolated into the past, the conflation leads to an underestimation of the total global emissions. Therefore, two different approaches have to be taken for the upper and lower bounds, differing for extrapolation forward in time or backwards in time. Backwards in time the lower bound estimate assumes minimal overlap and neglects this effect, while the higher bound estimate eliminates the scaling with GDP and population by normalizing with the global population and GDP of the current year. This means, that the total emissions grow parallel to the corresponding industrial production volume. Changes in GDP and Population on the other hand redistribute the total emissions, depending if the region underperforms or overperforms compared to the global average growth of population and GDP. As the growth with total production volume far outpaces population and GDP growth, this rarely leads to a decline in local product related emissions over time, but the effect still has to be noted. While extrapolating forwards in time these different approaches for lower bound and higher bound estimate invert, now ignoring the overlap in the higher bound estimate and overcompensating by scaling with the global real GDP and population in the lower bound.

2.5.6 Aqueous Film Forming Foams

POPE considers two factors for the temporal development of AFFF emissions: increasing prevalence of PFAS as well as supranational regulations and fadeouts. The latter are handled by country group and comprise regional total bans. The effects of upper limits for PFAS content of firefighting foams and changes in frequency of mandatory firefighting exercises are neglected. To capture the gradual implementation, increased air travel volumes, as well as the increasing air travel security standards

https://doi.org/10.5194/essd-2024-236
Preprint. Discussion started: 30 October 2024

developing over the years, a linear approximation is used from the start date to the previously approximated yearly emission values for the corresponding year. Further than that, there was not sufficient data available to substantiate a modelled decline or increase in use or PFAS-content of firefighting foams and both were therefore set constant. Note that also no opening or closing of airports is implemented, as the expected influence is expected to be minor, especially since even closed airports may still act as significant pollution sources (Linderoth et al., 2016).

3 POPE Emission Inventory

The result of the introduced assumptions and methods applied in the POPE emission model is the POPE emission inventory (available for download at permalink.aeris-data.fr/POPE), which contains global PFAS emission information for 5 different sectors, on a 0.5°equirectangular global grid, with a temporal resolution of one year, covering the years 1950 to 2020. Besides emissions into the atmosphere, the POPE emission inventory also contains emissions to rivers and the ocean by river-run off estimates.

The following sections explore the POPE emission inventory in detail. The results start with a general evaluation of the quality of POPE by comparing modelled river emissions with independent river measurements. This is followed by a comparison of global totals with the emission inventories by Prevedouros (Prevedouros et al., 2006) and Wang (Wang et al., 2014a). Finally, the spatial distribution is examined in further detail by showing the aggregated land emissions and the direct emissions to oceans, before the temporal development of the global and regional totals are shown.

3.1 Global Totals

As POPE combines the emission inventories by Prevedouros (Prevedouros et al., 2006) and Wang (Wang et al., 2014a) with other sources and socio-economic data, POPE is compared to these inventories to check its consistency with the original data. Figure 3 depicts this comparison for PFOA.

Figure 3 shows that between 1951 and 2002 the deviation of PFOA emissions in POPE relative to the other inventories is similar to the deviation of the chosen inventories relative to each other. The best guess scenario is compatible to all other estimates. This also holds true for the time period between 2003 and 2015. The upper limit of POPE is significantly lower than both upper limits of Wang et al. This may be attributed to the partial exclusion of secondary emissions by precursors and other indirect sources (Wang et al., 2014b) to reintroduce them with a different methodology, which produces lower estimates. With the fade-out of PFOA and the simultaneous switch to other PFAS, precursors gain in significance in recent years(Wang et al., 2017).

A similar picture is seen when comparing all PFCAs against the inventory of Wang et al. (Wang et al., 2014a) as in figure 4.

As the fluoropolymer production as biggest emission sector of POPE is build on Wang et al., both are expected to yield similar estimates. Differences concern mostly the emissions in product use and disposal, airport firefighting and precursors. Even with these different approaches and the inclusion of additional data and redistribution in space and time POPE is in general agreement with Wang et al. Essentially, also the relative contribution of each individual PFCA is very similar. Biggest

https://doi.org/10.5194/essd-2024-236
Preprint. Discussion started: 30 October 2024

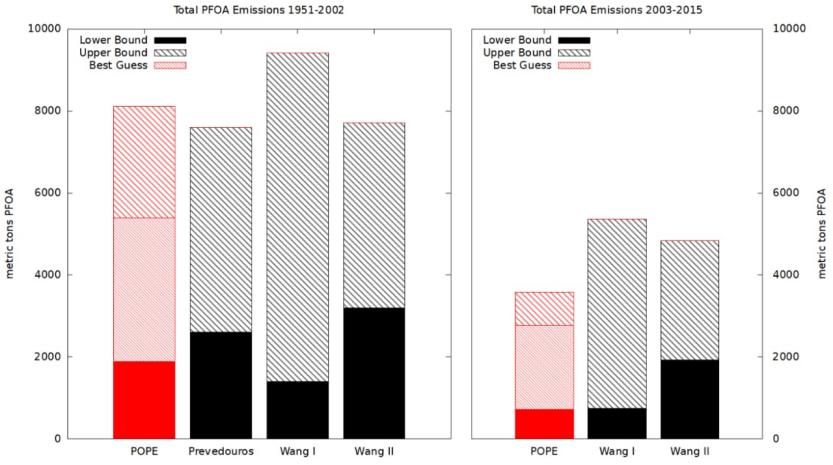

Figure 3. Comparison of total PFOA emissions for the upper boound, lower bound, and best guess of POPE for the time frames 1951-2002 and 2003-2015 to the emission estimnates provided in Prevedouros et al. (Prevedouros et al., 2006) and Wang et al. (Wang et al., 2014a). The red bar indicates the model.

outliers are an underestimation of PFOA as stated before, as well as a slight overestimation of PFNA. One explanation for the overestimation of PFNA is the inverse effect observable for PFOA in recent years, as PFNA is generally more prevalent in Europe and the United States compared to Asia (Langenbach et al., 2021). As the bias in the emission estimates for country group I is positive, while it is negative for the country group II this distribution leads to an overestimation in total. As POPE does not take into account more emission sources per se and uses identical numbers for fluoropolymer production this is mainly related to the estimates regarding the emissions during product use and disposal, which Wang accounts for differently.

3.2 Spatial distribution

This section presents the global gridded PFAS emissions over land as well as the expected river loads of PFOA to the global oceans.

Figure 5 depicts the aggregated total emissions in the best guess scenario for the time-period 1950- 2020 for each grid cell for PFOA, PFOS, 8:2-FTOH and HFPO-DA representative of PFCAs, PFSAs, FTOHs and substitutions respectively.

https://doi.org/10.5194/essd-2024-236
Preprint. Discussion started: 30 October 2024

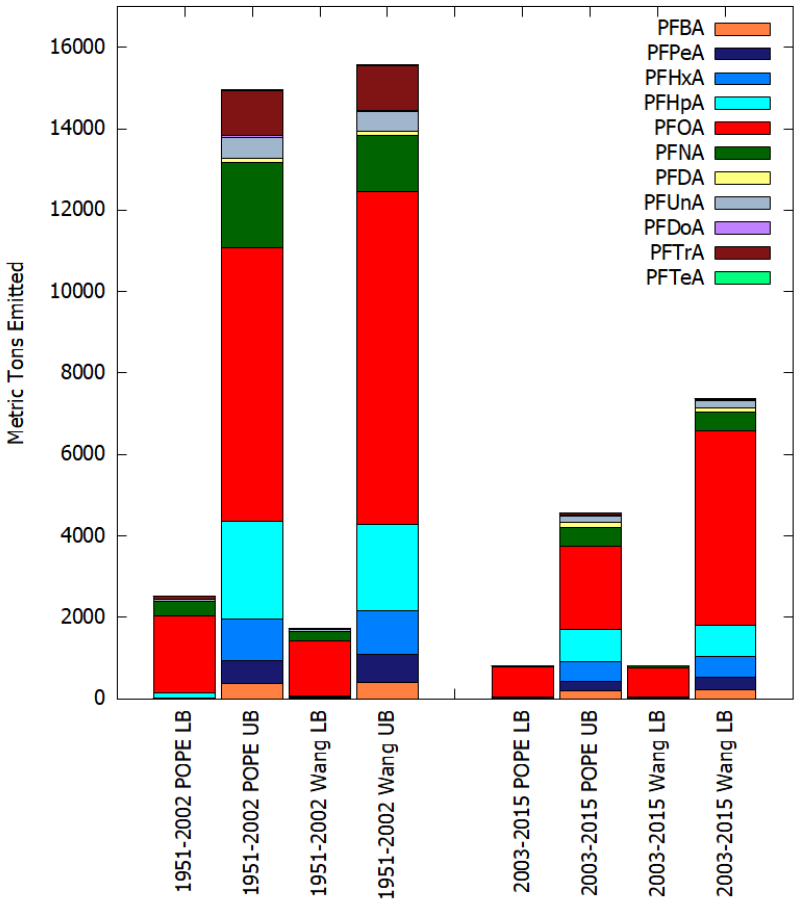

Figure 4. Comparison of the sum of all emissions of POPE for all PFCAs for the time frames 1951-2002 and 2003-2015 (Wang et al., 2014a)

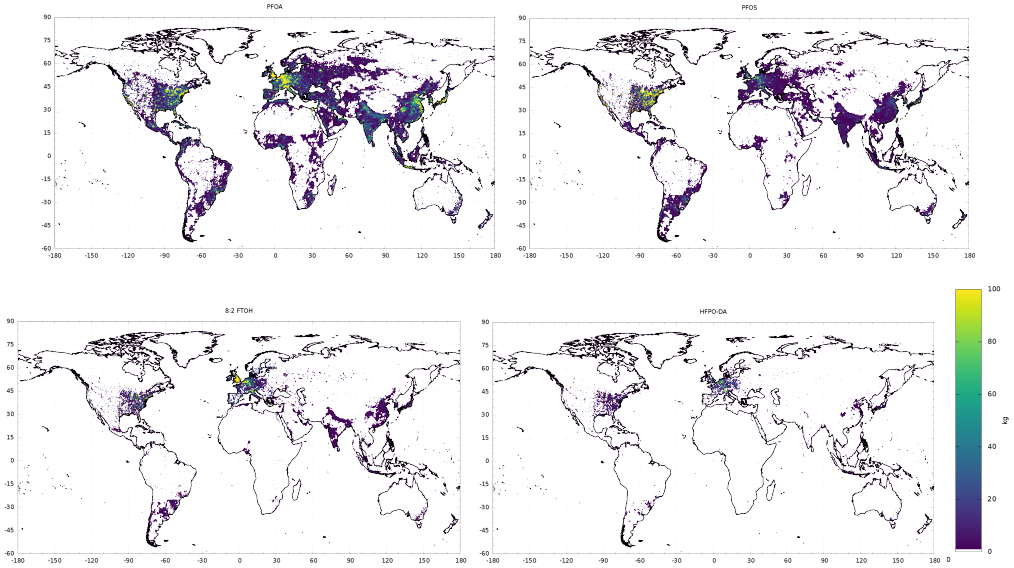

Figure 5. Global distribution of time-aggregated PFOA, PFOS, 8:2-FTOH and HFPO-DA emissions per grid cell during 1950-2020.The grid resolution is 0.5°x0.5°. The upper cut-off value is 100 kg, the lower cut off value is 1kg.

https://doi.org/10.5194/essd-2024-236
Preprint. Discussion started: 30 October 2024

Figure 5 reveals the direct influence of population density on PFOA and points out the main regions producing and using PFOA. These are central Europe, the east coast of the USA, Japan and the east coast of China. South and Central America, Africa and Oceania play a negligible role for the total emissions of PFOA. This map reflects the general expected distribution by GDP and population, whereas fluoropolymer production sites with significantly higher total aggregated emissions are in this case close to population centers. The importance of certain regions in relation to others changed over time, which will be discussed in section 3.3.

The emissions of PFOS are typically associated stronger with diffuse sources such as airport firefighting (Glüge et al., 2020). This is visible in figure 5 on a global scale, occuring widely with less hotspots. Also shown is the disparity of usage between the United States and other regions of the world. Within the US, again the east coast shows much higher emissions than the west coast.

As a replacement compound the total HFPO-DA emissions are in absolute numbers lower than legacy compounds up to now. It is mainly used in regions where PFOA has been phased out such as Europe, Japan, and the United States. This is reflected in the total aggregated emissions. Although the limited data suggest an incomplete picture, HFPO-DA emissions are more regionally contained than other PFAS. The production emissions dominate over the emissions over product lifecycles due to its novelty. The high availability for transport based on its physico-chemical properties may still lead to high concentrations distant to source regions.

8:2 FTOH is the most prevalent precoursor for PFOA. The distribution of the total aggregated emissions shown in Figure 5 show the prevalent usage in Europe with comparatively high emission loads the United Kingdom. These are mainly related to the usage of 8:2 -FTOH in advanced apparel manufacturing and treatment of surfaces. This emission distribution suggests that significant PFOA emissions can still be expected by precoursers alone.despite the upcoming total fade-out in the European Union.

3.3 Temporal Development

As PFAS were only produced in modern times and do not occur naturally, any emission inventory covering the years from 1950 onwards are temporally complete. Over the majority of this time span the dynamic is characterized by an increase in emissions.

But the relative importance of the individual regions was not the same over time. Important for the emission dynamics of legacy PFAS is the spatial shift of production from country group I to country group II after the year 2000. To illustrate how this dynamic is represented in POPE, Figure 6 shows the yearly emission of the best guess scenario for 5 geographical regions.

The major reduction of PFAS emissions in the United States and worldwide after 2000 is associated with multiple studies regarding the health risks of PFOA. These concerned the Dupont plant in Parkersburg, West Virginia, which up to this point was the largest emitter of PFAS in North America. The region with the second largest emission of PFAS during this time was Europe, however, the production and usage of products containing PFAS started significantly later. Japan behaved differently

https://doi.org/10.5194/essd-2024-236
Preprint. Discussion started: 30 October 2024

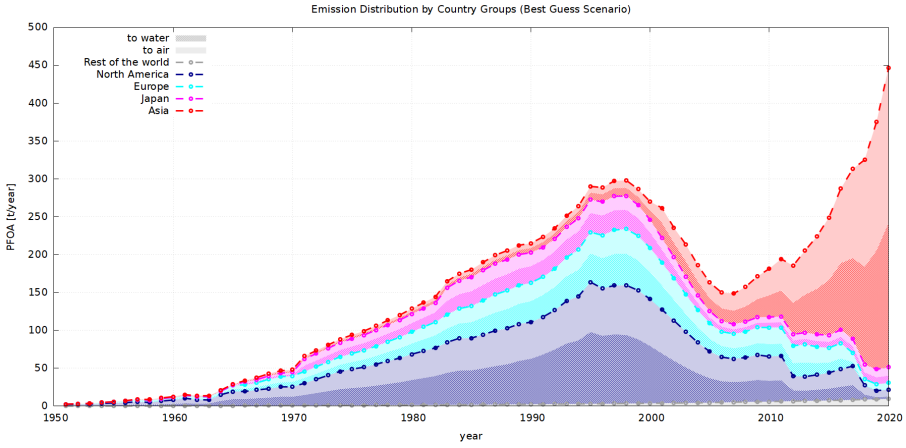

Figure 6. Total PFOA emissions by country group in the best guess scenario

than the rest of Asia, as it largely followed the trends of the United States and Europe, also showing a slow fade-out after 2000. During this time it is clearly visible that the global production of fluoropolymers shifted mainly to China. Additionally, the general increase of living standards in Asia reflected also in increased use and disposal of PFAS-related products.

4 Evaluation of the Emissions to Water

An advantage of the POPE emission inventory is the capability to model the release of PFAS into rivers and oceans consistently with the emissions to air. These riverine emissions were used to evaluate the POPE emission inventory. To calculate the PFAS river runoff into the oceans, the hydrological discharge (HD) model of Hagemann et al. (Hagemann et al., 2020) was used and compared to available concentration measurements in rivers.

4.1 Riverine transport model

The HD model calculates the lateral transport of water over the land surface to simulate discharge into the oceans. After its initial development (Hagemann and Dümenil, 1998), it has been validated and applied in many studies (Hagemann and Dümenil Gates, 2001)(Hagemann et al., 2020)(Hagemann and Stacke, 2022). The HD model requires gridded fields of surface and subsurface runoff as input with a temporal resolution of one day or higher. Similar to the experimental setup described in Hagemann and Stacke (Hagemann and Stacke, 2022), these were generated by the HydroPy global hydrology model. As meteorological forcing, Global Soil Wetness Project Phase 3 forcing data (Dirmeyer et al., 2006) were used from 1950-1978 and the WATCH Forcing Data based on ERA5 re-analysis (Cucchi et al., 2020) from 1979-2019. The HD model incorporates a framework for the transport of substances at the speed of the river flow. The calculated riverine emissions included in the POPE

https://doi.org/10.5194/essd-2024-236
Preprint. Discussion started: 30 October 2024

emission inventory were used as a direct input into the river, following the upper, lower and best guess estimates respectively. The emission volume was assumed to be constant over the year and homogeneous over any given gridcell. No chemical or physical transformation within the river is conducted as it is expected to play a minor role for river concentrations (Xu et al., 2021).

4.2 River concentrations

The calculated concentrations according to the POPE emission inventory and HD model are compared to several concentration measurements regarding the bias, trend along the river and to what extend the estimated bounds act as such. To quantify the relationship between the concentration measurement and the calculated bound according to POPE, the modified Root Mean Squared Normalized Error (RMSNE) is calculated for each study and each river individually according to

$$\text{RMSNE} = \sqrt{\frac{1}{n}\sum_i \left(\frac{c_{l,i} + \frac{1}{2}\Delta_i - c_{m,i}}{\frac{1}{2}\Delta_i}\right)^2}. \tag{9}$$

Here, $c_{m,i}$ is the concentration of the i-th measurement, $c_{l,i}$ the simulated concentration in the lower bound scenario at the position of the i-th measurement, n the number of measurements taken for that river in the corresponding study, and Δ_i the difference between the upper and lower bound scenario at the position of the i-th measurement. According to this metric, values below 1 indicate that all observed values fall in between the model bounds, while a value of RMSNE$= k$ signifies that the average difference between bound and measurement is $\frac{k^2-1}{2}$ times as large as the difference between upper and lower bound.

4.2.1 Trends along the River

Figure 7 shows PFOA concentrations in a selection of rivers focusing on rivers close to former and current fluropolymer-production sites, to capture trends along the river's length. This concerns six rivers, with two of them in the United States, Europe and China, respectively. These are the Rhine (Heydebreck et al., 2015) in the year 2013, the Elbe (Heydebreck et al., 2015) in the year 2014, the Cape Fear River (Sun et al., 2016) in 2013, the Ohio River (Galloway et al., 2020) in the year 2016, the Yangtze (Jin et al., 2009) in 2003 and the Xiaoquing in 2014 (Heydebreck et al., 2015). The rightmost values of each individual river are closest to the sea. Note, that the distance between two measurements may be less than the resolution of the emission-model and therefore, for both the same upper and lower bound may apply. Also note, that the measurements by Sun et al. were mostly under the quantification limit, whereas the measurements of the Xiaoquing by Heydebreck et al. yielded much higher concentrations than the calibration range, leading to potentially higher uncertainty.

https://doi.org/10.5194/essd-2024-236
Preprint. Discussion started: 30 October 2024

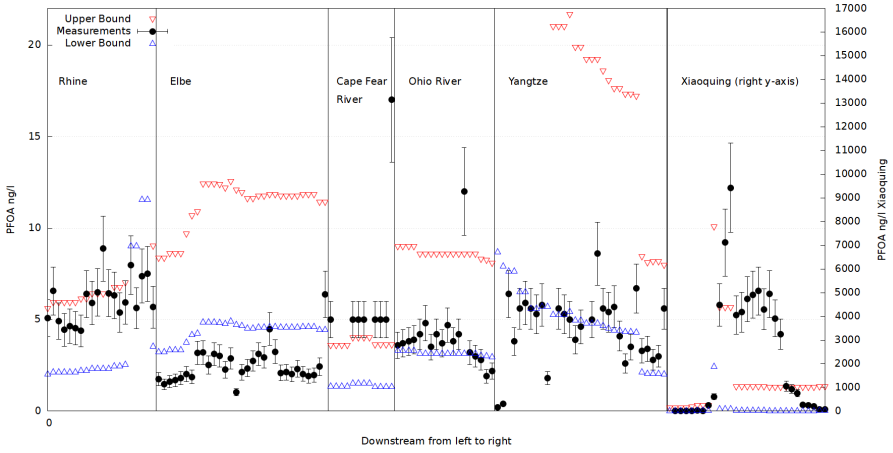

Figure 7. Overview of several river concentration measurements by Sun et al.(Sun et al., 2016), Pétré et al. (Pétré et al., 2022), Heydebreck et al. (Heydebreck et al., 2015) and Jin et al. (Jin et al., 2009) in comparison with the upper and lower bound estimation by POPE. The rightmost values are closest to the sea.

POPE and the measurements show similar trends over the length of the rivers. Deviations seem to be mostly in form of a consistent bias over the whole river length for all rivers. Also the general trend indicating the growth of taken up emission relative to the increase in water mass is mostly clear. This is very much visible for the Rhine, Elbe, Ohio River and Yangtze. Individual extreme values as for example directly at the plant in the Ohio River, or specific high points at the Elbe or Cape-Fear River are smoothed out due to the nature of the model. Differences in the trend seem comparatively lower to the overall bias. This may suggests large scale distributional errors, affecting the attribution of emissions to whole regions or sectors rather than large local fluctuations due to inaccurately placed point sources or wrong attribution of production volume.

Large relative and the largest absolute deviation for the Xiaoquing River suggest that the modelled emissions in its watershed are underestimated in the POPE emission inventory. In the regions of highest concentration near the plant, the upper bound falls short by an order of magnitude. Downstream the concentration in the model falls to a much lower level than the measurements suggest. One possible explanation may be the influence of atmospheric deposition of emissions to air, which increase the river concentration as a whole and may exend the influence of the production plant downstream. Other explanations may be an underestimation of the total emissions in Asia or country group II respectively. Relative overestimation as with the Yangtze river on the other hand suggest again rather distributional errors. Based on the distribution method in China this may hint to the fact, that the relative impact of population as emittent, combined with population and GDP as a proxy underestimates the impact of few high emission point sources. Furthermore, this can be impacted by the assumption that the use of recovery methods during the production process is on the same level as reported for e.g. the United States. This assumption was made due to a supposed strong economic motivation in reusing processing aids. Assuming loss fractions as reported for the United States in the 50s and 60s as in figure 2 could increase PTFE-production emissions by a factor of about 10 and therefore explain

https://doi.org/10.5194/essd-2024-236
Preprint. Discussion started: 30 October 2024

part of the missing emissions and deviation from observations.

650

4.2.2 Average Error and Bias

Shown in table 5 are the RMSNE and the mean difference between measured concentration and the modelled concentration for the best guess estimate. Additionally shown are the Pearson correlation coefficients r to assess how well the model captures the trend along the river, for all rivers where multiple measuring points are available

655 The results show varied picture. This is attributed to a multitude of factors, which may be related to the emission inventory but also due to the comparison of a snapshot in time that the river measurements provide to averaged model results, or processes in the river not accounted for, intra-annual variations in production emissions as well as a general environmental retardation. This also becomes visible in the general better agreement for larger rivers for which the relative influence of these variations is smaller. Additionally, there is a better agreement for rivers which are well researched as the Rhine and the Ohio River.

660 The model tends to overestimate emissions to rivers without major production sites, with positive biases and RMNSEs significantly larger than one, as for example at the Haw River or Daugava. There, the emissions are mostly impacted by the smaller manufacturing industry point sources for which size data is not avaialable but may hint at smaller production volumes and emissions.

On the other hand, PFAS concentrations in rivers which are situated near industries which are not included in the model may 665 deviate significantly. This is for example visible for the Danube, similar to the results of Lindim et al. (Lindim et al., 2015a). This is exacerbated by the broad approach of industry sectors where corresponding sectors with high average PFAS emissions like apparel manufacturing may in reality be dominated by a few sites with relevant production of e.g. outdoor apparel, while most sites emit little to no PFAS at all (Glüge et al., 2020).

670

The correlation coefficients r of the measured concentrations to the POPE best guess emission estimates measures the agreement in dilution and emission input for both. These are mostly positive in the range of r = 0.25 to 0.75. Most of the correlation coefficients show, that the general trend of increasing concentration with increasing emission sources and decreasing concentration with increasing runoff is captured. The lowest value of -0.14 is for the Xiaoquing River. Here not only the absolute value is 675 not captured, but also the trend reverts. This may suggest differing positions of the actual emission input and the modelled input.

The calculated biases are mostly in the order of magnitude of the observed concentrations. They hint at a distribution problem with an underestimation of Chinese single point sources and an overestimation of European and North-American emissions. As POPE is neglecting emission sources, as for example several possible precursors, and showed lower estimates for diffuse 680 emissions than previous emission estimations a negative bias would have been expected. This may mean, that other factors such as loss fractions or the used average emission per person are too high. A fraction of the emissions may also be wrongly

https://doi.org/10.5194/essd-2024-236
Preprint. Discussion started: 30 October 2024

Open Access Earth System Science Data Discussions

Table 5. The modified Root Mean Squared Normalized Error (RMSNE), correlation coefficient r and the bias between measurements and simulated values in comparison to several studies.

River	Source	year	RMSNE	r	Bias [ng/l]
Cape Fear River	Sun et al. (Sun et al., 2016)	2013	1.51	-	-4.29
Cape Fear River	Pétré et al. (Pétré et al., 2022)	2018	1.77	-	2.93
Cape Fear River	Pétré et al. (Pétré et al., 2022)	2019	5.43	-	4.92
Cape Fear River	Pétré et al. (Pétré et al., 2022)	2020	3.65	-	3.90
Dalälven	Mclachlan et al. (Mclachlan et al., 2007)	2005	1.90	-	0.45
Danube	JSD3 (Liška et al., 2015)	2013	1.41	0.59	-6.27
Danube	Mclachlan et al. (Mclachlan et al., 2007)	2005	0.98	-0.09	-18.52
Daugava	Mclachlan et al. (Mclachlan et al., 2007)	2006	13.48	-	1.89
Elbe	Heydebreck et al. (Heydebreck et al., 2015)	2014	1.72	0.55	5.80
Elbe	Mclachlan et al. (Mclachlan et al., 2007)	2005	2.06	-	3.05
Ems	Heydebreck et al. (Heydebreck et al., 2015)	2013	1.17	0.29	2.04
Haw River	Pétré et al. (Pétré et al., 2022)	2019	17.50	0.75	13.41
Haw River	Pétré et al. (Pétré et al., 2022)	2020	10.29	0.62	8.91
Kalix	Mclachlan et al. (Mclachlan et al., 2007)	2005	4.54	-	0.59
Loire	Mclachlan et al. (Mclachlan et al., 2007)	2006	1.56	0.35	1.44
Oder	Mclachlan et al. (Mclachlan et al., 2007)	2005	1.45	-	1.47
Ohio River	Galloway et al. (Galloway et al., 2020)	2016	1.02	0.72	1.81
Po	Mclachlan et al. (Mclachlan et al., 2007)	2006	0.86	-	68.25
Quadalquivir	Mclachlan et al. (Mclachlan et al., 2007)	2006	1.62	-	-11.28
Raisin River	Michigan DEQ (Division, 2019)	2018	2.31	0.25	0.71
Rhine	Heydebreck et al. (Heydebreck et al., 2015)	2013	0.71	0.74	3.14
Rhine	Mclachlan et al. (Mclachlan et al., 2007)	2006	4.13	-	0.25
Seine	Mclachlan et al. (Mclachlan et al., 2007)	2006	1.12	-	1.97
Thames	Mclachlan et al. (Mclachlan et al., 2007)	2006	2.90	-	-4.06
Vindelälven	Mclachlan et al. (Mclachlan et al., 2007)	2005	5.47	-	0.47
Vistula	Mclachlan et al. (Mclachlan et al., 2007)	2005	1.15	-	-5.89
Weser	Heydebreck et al. (Heydebreck et al., 2015)	2013	1.82	0.43	4.05
Xiaoquing	Heydebreck et al. (Heydebreck et al., 2015)	2014	4.73	-0.14	-4341.00
Yangtze	Jin et al. (Jin et al., 2009)	2003	1.35	0.31	4.93

distributed, for example from country group II to country group I, which is mainly based on population and GDP Asia might be wrongly attributed to Europe and the USA. Factors like a bias in certain input data, as for example the per person emission, might also cause this trend.

https://doi.org/10.5194/essd-2024-236
Preprint. Discussion started: 30 October 2024

4.2.3 Total loads

For most environmental concerns the sum of PFAS is the relevant quantity. Figure 8 shows how the sum of PFAS in POPE, transported with the HD Modell, relates to the measured sum of PFAS in the studies from table 5. The shown ranges are spatio-temporal ranges covering all measurements over the whole river length. All model data relates to the best guess scenario and the range over all corresponding gridcells with the median indicated by the black bar.

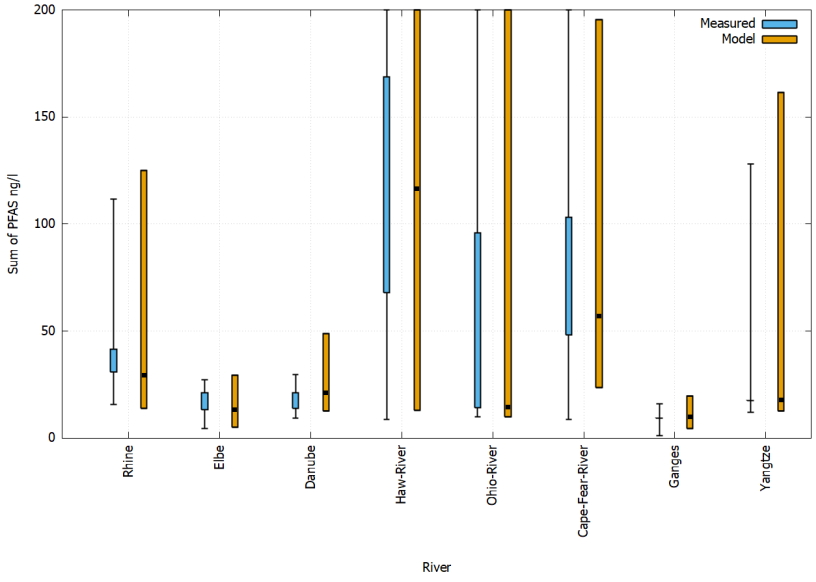

Figure 8. Comparison of the range of the sum of all PFAS in selected rivers with the best guess estimate of POPE. The whisker-bars indicate the measured quartiles, where available. The black line in the modelled results indicates the median concentration of all corresponding gridcells.

There is high overlap between the measured ranges and the ranges based on the POPE emission inventory. As the correlation factors indicate measured and calculated values do not always agree in space and time. The high temporal variation of the river loads is not well represented in the model. The shown bias is not identical for all rivers. Concentrations in heavily industrialised river basins are underestimated while concentrations in basins with less industry are overestimated. The general concentration range is captured adequately, although the coarse resolution of POPE tends to smooth local high emissions. At the same time the used gridcell mask is in total bigger than the corresponding rivers leading to the inclusion of a wider range of values. Adding all substances improves the agreement suggesting non-systematic errors canceling each other out. which is why the relative contribution of individual PFAS will be assessed later.

https://doi.org/10.5194/essd-2024-236
Preprint. Discussion started: 30 October 2024

4.2.4 Relative Contributions to the Total

Apart from the total concentration in any given river it is of interest to compare the relative PFAS fractions of the POPE emission inventory with concentrations measurements in rivers. Figure 9 shows this fraction of the total PFAS load averaged over all measurements, or the corresponding gridcells respectively. These fractions consider only substances found in both POPE and the study at hand meaning the shown substances do not necessarily represent the most important contributors to the total PFAS load in each river.

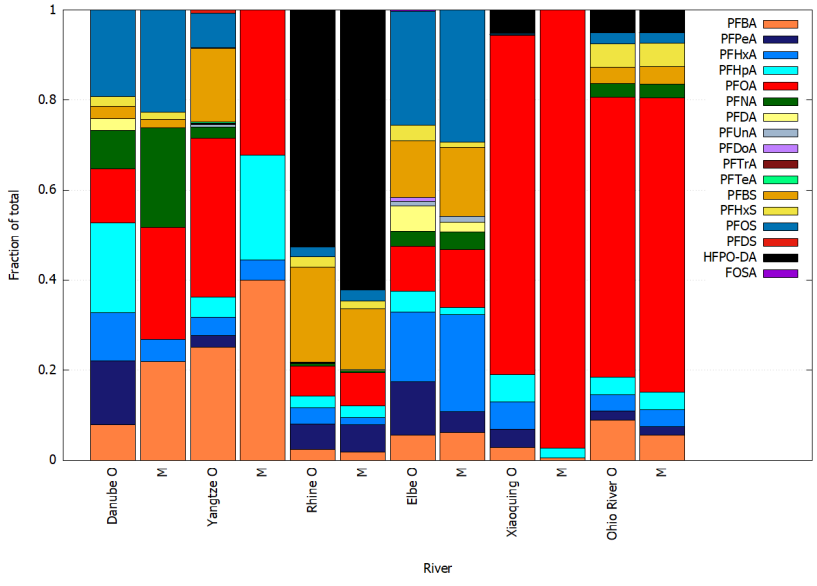

Figure 9. Relative fraction of all PFAS considered by POPE and the respective studies for a selection of rivers. O indicates an observation, M designates the corresponding modelled result.The order of substances in the legends corresponds to the inverse vertical order of fractions.

The best agreement is again found for the most extensively studied rivers, the Ohio River and the Rhine and the most extensively studied PFAS of PFOA and PFOS. The Rhine is especially of interest as it is influenced heavily by the replacement of PFOA by HFPO-DA. Even though the absolute PFAS concentrations in the Rhine tend to exceed the upper bound the fraction of HFPO-DA and therefore the replacement factor used in POPE is compatible with the measurements. The relative fraction of PFBA on the other hand may hint at a distribution error between countries. The Danube and Yangtze show large differences especially for PFBA and PFNA. The latter was already observable in the totals and is most likely associated with an inaccurate split between the two associated Fluoropolymers PTFE and PVDF. Similar distributional deviations as for PFBA can also be observed for PFHpA which is assumed to be dominantly used in Asia while measurements show an unknown source near the Danube. The two chinese Rivers Yangtze and Xiaoquing suffer again from the insufficient data on used PFAS mainly due to the simplification that country group II uses mostly legacy PFAS while the measurements show that the usage is broader than anticipated. Additionally, some unknown industries not associated with PFSA usage in POPE seem to have a big

https://doi.org/10.5194/essd-2024-236
Preprint. Discussion started: 30 October 2024

715 influence on the Yangtze basin, which is not considered in POPE. These gaps pose opportunities for improvement of POPE with more accurate industrial data in country group II.

4.3 Ocean Emissions

Many relevant PFAS are acids or alcohols, some with very low acid dissociation constants (Buck et al., 2011) like PFOA, they are expected to remain dissolved, once they were in contact with water masses, cloud droplets or water soluble aerosol
720 particles. Therefore the global oceans are highly relevant for the long term fate of PFAS. Table 6 lists the total calculated PFAS load by rivers over the time-period 1951 to 2020 to the Arctic Ocean (AO), North Atlantic (NA), South Atlantic (SA), North Pacific (NP), South Pacific (SP), Indian Ocean (IO), Mediterranean Sea (MS), North- and Baltic Sea (NBS) in the upper bound scenario, as simulated by the HD model based on POPE emissions. Figure 10 depicts the river discharges of PFOA into the Arctic Ocean, the North Atlantic Ocean, the South Atlantic Ocean, the North Pacific Ocean, the South Pacific Ocean, the
725 Indian Ocean, the Mediterranean Sea and the North- and Baltic Sea over time for the upper bound scenario. Note that this only contains riverine emissions without any atmospheric transport and without exchange between oceans. This means, for example high levels of PFAS in the North Atlantic are expected to cause a high PFAS burden on the south Pacific and the Arctic ocean, due to interoceanic exchange. This reemphasizes the need for transport modelling to assess the long term fate of PFAS in the oceans and atmosphere.

Table 6. Total PFAS river load [t] for the time period 1950-2020 and relative fractions [%] released to the Arctic Ocean (AO), North Atlantic (NA), South Atlantic (SA), North Pacific (NP), South Pacific (SP), Indian Ocean (IO), Mediterranean Sea (MS), North- and Baltic Sea (NBS) in the upper bound scenario

Ocean	AO	NA	SA	NP	SP	IO	MS	NBS
Total load [t]	150	24700	416	23580	70	1554	10766	5708
Relative fraction [%]	0.2	36.9	0.6	35.2	0.1	2.3	16.1	8.5

730 As shown in Table 6 again the northern hemisphere is far more affected by PFAS pollution than the southern hemisphere. The North Atlantic and North Pacific received the majority of PFAS loads. Based on Figure 6 large east-west concentration gradients are expected in both seas. Even small marginal seas, like the Mediterranean Sea, are subject to significant pollution.

The pictured PFAS fluxes into the oceans in figure 10 mirror the general trend of the regions. However a significant flux of PFOA to the North Atlantic mainly by precursors and emitted through PFOA containing products persists. It becomes
735 apparent, that the majority of the emissions from North America enter the North Atlantic rather than the North Pacific, while the distinction between the Mediterranean and the North- and Baltic Sea shows, that the significantly smaller contribution of Europe splits roughly equally between these two. The contributions of Europe to the North Atlantic PFOA concentrations via the direct river runoff is minor and comes only into play in exchange with the north sea. Over the whole time period, the Arctic Ocean and the southern Oceans are only slightly affected by direct river discharges. The concentration levels found for example

https://doi.org/10.5194/essd-2024-236
Preprint. Discussion started: 30 October 2024

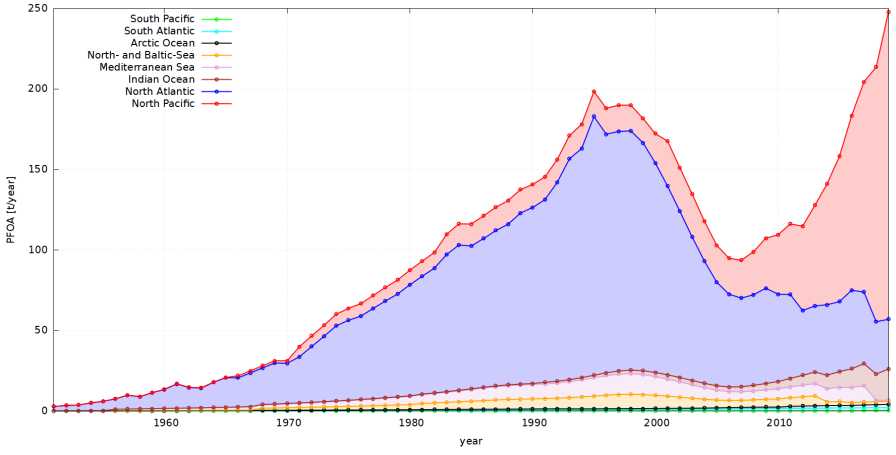

Figure 10. Total PFOA emissions to oceans in the upper bound scenario

by Joerss et al. (Joerss, 2020) or Boitsov et al. (Boitsov et al., 2024) may therefore be closer related to atmospheric transport and the exchange with neighboring oceans.

5 Conclusions

The PFAS emission model and inventory POPE builds on existing global inventories by disaggregating decadal total emission loads with socioeconimc proxies and industrial data. POPE collects several local and regional emission estimations to build one consistent scenario capable dataset, distinguishing between 5 different sectors and two compartments in a 0.5°resolution gridded model ready format. Upper and lower bounds as well as a best guess estimate are provided. POPE extra- and interpolates existing production volumes and couples use and disposal emissions to these production estimates to obtain an annual complete inventory from 1950 to 2020. POPE extends methods used for emission estimations of legacy PFAS to precursors and novel PFAS to get one step closer to a complete picture of PFAS emission. The consistent method is easily expandable to cover more PFAS as soon as the necessary data is available.

The POPE emission inventory is compatible with emission inventories it builds upon but expects mostly slightly lower emissions based on its different approach to use and disposal of PFAS products. As depicted in in Figure 6 and Table 6 (Section 3.3) POPE is able to capture the main dynamics concerning the spatial and temporal trends in PFAS emissions:

- North America and to a lesser extent Europe and Japan dominate the PFAS emissions in the twentieth century-
- A temporal shift of emissions from Europe and North America to Asia starts after the year 2000.
- Significant emissions remains even after the total or partial fade-out of legacy PFAS such as PFOA and PFOS.

https://doi.org/10.5194/essd-2024-236
Preprint. Discussion started: 30 October 2024

Different application profiles as well as national differences in the prevalence of different PFAS are captured by the POPE emission inventory. Legacy PFAS can be exemplary to estimate emissions for precursors and novel compounds PFAS.

POPE has been evaluated with independent data based on PFAS concentrations in major rivers (section 4). Although the emissions to water paint an incomplete picture and the comparison of averaged model results with concentration measurements has limited informative value, these results hint towards the possible usefulness of the POPE emission inventory. As expected, the best agreement regarding concentration measurements was found for Europe and the United States, as the model relies heavily on data from these regions (See Table 5 and figure 7). Found biases are inconsistent showing no trend of an total over- or underestimations. The trend along rivers indicates a successful source apportionment. Long time series in European rivers could help to evaluate the temporal quality of the emission inventory. In Asia, PFAS emissions seem to be generally underestimated, while some species found in rivers cannot be attributed to a source at all. The POPE model as a whole could be improved by more data on the location, production volume and expected loss fractions of fluoropolymer production sites in Asia, as well as better profiles which PFAS are in use and in which industries. For the southern hemisphere, there is no independent data for evaluation available.

Deviations in the evaluation could most of the time be attributed to a too homogeneous distribution, limited either by the model resolution or the necessary reliance on proxies. A two tracked approach as taken for non fluoropolymer industries in Europe with locations and employee numbers is leads to a promising emission estimation. Bottom-up estimated emissions exhibit better agreement of measured concentration and modelled concentration as shown in Figure 9.
For all purposes, the inclusion of more individual industrial sites with associated production volumes and loss fractions is needed. Studies similar to the ones already performed for PFOA and PFOS on major industrial sites and airports for emerging PFAS such as GenX and Adona could help to represent their emissions more accurately. More consistent reporting of production volumes and in cases of shifts between compounds replacement factors are needed to obtain useful emission values for GenX and Adona. FOSA also shows significant knowledge gaps regarding emissions considering its relative importance for the formation of PFOS.

.

The spatial and temporal trends exhibited in the POPE emission inventory reemphasize the relevance of numerical multi compartment transport modelling. With the growing importance of product related emissions and precursors it is clear that even with strict PFAS regulations in place, significant emissions will still occur over extended time periods. The expected concentration gradient between regions poses the question of the importance of long range atmospheric and marine transport to remote locations like the Arctic. The geographical shift in industrial production leads to competing influences of legacy emissions and imported emissions from other countries.

https://doi.org/10.5194/essd-2024-236
Preprint. Discussion started: 30 October 2024

POPE can support advancing multi-compartment transport modeling with consistent global emission data for PFAS, distinguishing between emissions to rivers/oceans and emissions to the atmosphere. This enables models to identify source-receptor relationships for PFAS pollution and to simulate different scenarios to predict its transport and concentration in multiple compartments. As the POPE emission inventory begins with the first production of PFAS in 1950 chemistry transport models can be run independently of initial conditions. Furthermore, it is possible to perform simulations in non-equilibrium states, capturing the dynamics of increasing production, followed by a local fade-out and spatial shift of global PFAS emissions. The POPE framework is applicable to other PFAS not yet considered and will be extended as data becomes available.

Code and data availability. The code and data of the POPE Emission model is available at Zenodo (https://doi.org/10.5281/zenodo.12783504) (Simon, 2024) distributed under Creative Commons 4.0 Attribution. Alternatively the POPE emission inventory is also publicly available in GEIA's (Global Emission InitiAtive) ECCAD data portal: (https://permalink.aeris-data.fr/POPE)(Simon, 2024).

Author contributions. Details of each author with their contribution in this paper is as under:

Pascal Simon:
Conceptualization, Investigation, Methodology, Formal Analysis, Software: POPE, Writing – Original Draft

Martin Otto Paul Ramacher:
Conceptualization, Methodology, Validation, Writing - Review and Editing

Stefan Hagemann:
Software: HD-model, Validation, Writing - Review and Editing

Volker Matthias:
Conceptualization, Writing - Review and Editing

Hanna Joerss:
Conceptualization, Validation, Writing - Review and Editing

https://doi.org/10.5194/essd-2024-236
Preprint. Discussion started: 30 October 2024

825 Johannes Bieser:

Conceptualization, Methodology, Supervision, Writing - Review and Editing

Competing interests. I declare that neither I nor my co-authors have any competing interests.

Acknowledgements. We want to thank Professor Corinna Schrum for supervision, as well as Hugo Denier van der Gon and Sabine Darras for the possibility to distribute the POPE model via ECCAD (Emissions of atmospheric Compounds and Compilation of Ancillary Data), the
830 GEIA Global Emission InitiAtive's data portal, which is part of AERIS , the French data service for Atmosphere. Moreover, we thank Ian Cousins for scientific discussions and his feedback regarding the model and manuscript. All research has been carried out as part of the I2B project MCMEE funded by the Helmholtz-Zentrum Hereon

https://doi.org/10.5194/essd-2024-236
Preprint. Discussion started: 30 October 2024

References

Ahrens, L.: Polyfluoroalkyl Compounds in the Marine Environment – Investigations on their Distribution in Surface Water and Temporal Trends in Harbor Seals (, 2009.

Ahrens, L., Norström, K., Viktor, T., Cousins, A. P., and Josefsson, S.: Stockholm Arlanda Airport as a source of per- and polyfluoroalkyl substances to water, sediment and fish, Chemosphere, 129, 33–38, https://doi.org/10.1016/j.chemosphere.2014.03.136, 2015.

Armitage, J., Cousins, I. T., Buck, R. C., Prevedouros, K., Russell, M. H., Macleod, M., and Korzeniowski, S. H.: Modeling global-scale fate and transport of perfluorooctanoate emitted from direct sources, Environmental science & technology, 40, 6969–6975, https://doi.org/10.1021/ES0614870, 2006.

Armitage, J. M., Macleod, M., and Cousins, I. T.: Modeling the global fate and transport of perfluorooctanoic acid (PFOA) and perfluorooctanoate (PFO) Emitted from direct sources using a multispecies mass balance model, Environmental Science and Technology, 43, 1134–1140, https://doi.org/10.1021/es802900n, 2009.

Bieser, J. and Ramacher, M. O. P.: Multi-compartment Chemistry Transport Models, Springer Proceedings in Complexity, pp. 119–123, https://doi.org/10.1007/978-3-662-63760-9_18/COVER, 2021.

Bieser, J., Aulinger, A., Matthias, V., Quante, M., and Builtjes, P.: SMOKE for Europe-adaptation, modification and evaluation of a comprehensive emission model for Europe, Geoscientific Model Development, 4, 47–68, https://doi.org/10.5194/gmd-4-47-2011, 2011.

Boitsov, S., Bruvold, A., Hanssen, L., Jensen, H. K., and Ali, A.: Per- and polyfluoroalkyl substances (PFAS) in surface sediments of the North-east Atlantic Ocean: A non-natural PFAS background, Environmental Advances, 16, https://doi.org/10.1016/j.envadv.2024.100545, 2024.

Brandsma, S. H., Koekkoek, J. C., van Velzen, M. J., and de Boer, J.: The PFOA substitute GenX detected in the environment near a fluoropolymer manufacturing plant in the Netherlands, Chemosphere, 220, 493–500, https://doi.org/10.1016/J.CHEMOSPHERE.2018.12.135, 2019.

Brennan, N. M., Evans, A. T., Fritz, M. K., Peak, S. A., and von Holst, H. E.: Trends in the regulation of per-and polyfluoroalkyl substances (PFAS): A scoping review, International Journal of Environmental Research and Public Health, 18, https://doi.org/10.3390/ijerph182010900, 2021a.

Brennan, N. M., Evans, A. T., Fritz, M. K., Peak, S. A., and von Holst, H. E.: Trends in the regulation of per-and polyfluoroalkyl substances (PFAS): A scoping review, International Journal of Environmental Research and Public Health, 18, 10 900, https://doi.org/10.3390/IJERPH182010900/S1, 2021b.

Buck, R. C., Franklin, J., Berger, U., Conder, J. M., Cousins, I. T., Voogt, P. D., Jensen, A. A., Kannan, K., Mabury, S. A., and van Leeuwen, S. P.: Perfluoroalkyl and polyfluoroalkyl substances in the environment: Terminology, classification, and origins, Integrated Environmental Assessment and Management, 7, 513–541, https://doi.org/10.1002/ieam.258, 2011.

Chambers, J.: Hybrid gridded demographic data for the world, 1950-2020, https://doi.org/10.5281/ZENODO.3768003, 2020.

Conder, J. M., Hoke, R. A., De Wolf, W., Russell, M. H., and Buck, R. C.: Are PFCAs bioaccumulative? A critical review and comparison with regulatory criteria and persistent lipophilic compounds, Environmental Science and Technology, 42, 995–1003, https://doi.org/10.1021/ES070895G, 2008.

Cousins, I. T., Kong, D., and Vestergren, R.: Reconciling measurement and modelling studies of the sources and fate of perfluorinated carboxylates, Environmental Chemistry, 8, 339–354, https://doi.org/10.1071/EN10144, 2011.

https://doi.org/10.5194/essd-2024-236
Preprint. Discussion started: 30 October 2024

Cousins, I. T., Dewitt, J. C., Glüge, J., Goldenman, G., Herzke, D., Lohmann, R., Ng, C. A., Scheringer, M., and Wang, Z.: The high persistence of PFAS is sufficient for their management as a chemical class, Environmental Science: Processes and Impacts, 22, 2307–2312, https://doi.org/10.1039/d0em00355g, 2020.

Cucchi, M., P. Weedon, G., Amici, A., Bellouin, N., Lange, S., Müller Schmied, H., Hersbach, H., and Buontempo, C.: WFDE5: Bias-adjusted ERA5 reanalysis data for impact studies, Earth System Science Data, 12, 2097–2120, https://doi.org/10.5194/ESSD-12-2097-2020, 2020.

Dalmijn, J., Glüge, J., Scheringer, M., and Cousins, I. T.: Emission inventory of PFASs and other fluorinated organic substances for the fluoropolymer production industry in Europe, Environmental Science: Processes and Impacts, 26, 269–287, https://doi.org/10.1039/d3em00426k, 2023.

De Silva, A. O., Armitage, J. M., Bruton, T. A., Dassuncao, C., Heiger-Bernays, W., Hu, X. C., Kärrman, A., Kelly, B., Ng, C., Robuck, A., Sun, M., Webster, T. F., and Sunderland, E. M.: PFAS Exposure Pathways for Humans and Wildlife: A Synthesis of Current Knowledge and Key Gaps in Understanding, Environmental Toxicology and Chemistry, 40, 631–657, https://doi.org/10.1002/ETC.4935, 2021.

Dirmeyer, P. A., Gao, X., Zhao, M., Guo, Z., Oki, T., and Hanasaki, N.: GSWP-2: Multimodel Analysis and Implications for Our Perception of the Land Surface, Bulletin of the American Meteorological Society, 87, 1381–1398, https://doi.org/10.1175/BAMS-87-10-1381, 2006.

Division, W. R.: River Raisin Surface Water PFAS Follow-up Investigation September 2019, pp. 2–5, 2019.

EC: Proposal COM/2022/540 for a Directive of the European Parliament and of the Council amending Directive 2000/60/EC establishing a framework for Community action in the field of water policy, Directive 2006/118/EC on the protection of groundwater against pollution and deterioration and Directive 2008/105/EC on environmental quality standards in the field of water policy, 2022.

EC: Industrial Reporting under the Industrial Emissions Directive 2010/75/EU and European Pollutant Release and Transfer Register Regulation (EC) No 166/2006, 2023.

EPA, U.: Facility Registry Service https://www.epa.gov/frs, 2023.

Filipovic, M., Berger, U., and Mclachlan, M. S.: SUPPORTING INFORMATION Mass balance of perfluoroalkyl acids in the Baltic Sea, Tech. rep.

Filipovic, M., Berger, U., and McLachlan, M. S.: Mass balance of perfluoroalkyl acids in the Baltic sea, Environmental Science and Technology, 47, 4088–4095, https://doi.org/10.1021/es400174y, 2013a.

Filipovic, M., Berger, U., and McLachlan, M. S.: Mass balance of perfluoroalkyl acids in the Baltic sea, Environmental Science and Technology, 47, 4088–4095, https://doi.org/10.1021/es400174y, 2013b.

Filipovic, M., Woldegiorgis, A., Norström, K., Bibi, M., Lindberg, M., and Österås, A. H.: Historical usage of aqueous film forming foam: A case study of the widespread distribution of perfluoroalkyl acids from a military airport to groundwater, lakes, soils and fish, Chemosphere, 129, 39–45, https://doi.org/10.1016/j.chemosphere.2014.09.005, 2015.

Galloway, J. E., Moreno, A. V., Lindstrom, A. B., Strynar, M. J., Newton, S., May, A. A., May, A. A., Weavers, L. K., and Weavers, L. K.: Evidence of Air Dispersion: HFPO-DA and PFOA in Ohio and West Virginia Surface Water and Soil near a Fluoropolymer Production Facility, Environmental Science and Technology, 54, 7175–7184, https://doi.org/10.1021/acs.est.9b07384, 2020.

Gebbink, W. A. and van Leeuwen, S. P.: Environmental contamination and human exposure to PFASs near a fluorochemical production plant: Review of historic and current PFOA and GenX contamination in the Netherlands, https://doi.org/10.1016/j.envint.2020.105583, 2020.

Glüge, J., Scheringer, M., Cousins, I. T., Dewitt, J. C., Goldenman, G., Herzke, D., Lohmann, R., Ng, C. A., Trier, X., and Wang, Z.: An overview of the uses of per- And polyfluoroalkyl substances (PFAS), Environmental Science: Processes and Impacts, 22, 2345–2373, https://doi.org/10.1039/d0em00291g, 2020.

https://doi.org/10.5194/essd-2024-236
Preprint. Discussion started: 30 October 2024

Goldenman, G., Fernandes, M., Holland, M., Tugran, T., Nordin, A., Schoumacher, C., and McNeill, A.: The cost of inaction, TemaNord, Nordic Council of Ministers, Copenhagen, ISBN 9789289360654, https://doi.org/10.6027/TN2019-516, 2019.

Guelfo, J. L., Korzeniowski, S., Mills, M. A., Anderson, J., Anderson, R. H., Arblaster, J. A., Conder, J. M., Cousins, I. T., Dasu, K., Henry, B. J., Lee, L. S., Liu, J., McKenzie, E. R., and Willey, J.: Environmental Sources, Chemistry, Fate, and Transport of Per- and Polyfluoroalkyl Substances: State of the Science, Key Knowledge Gaps, and Recommendations Presented at the August 2019 SETAC Focus Topic Meeting, Environmental Toxicology and Chemistry, 40, 3234–3260, https://doi.org/10.1002/ETC.5182, 2021.

Hagemann, S. and Dümenil, L.: A parametrization of the lateral waterflow for the global scale, Climate Dynamics, 14, 17–31, https://doi.org/10.1007/S003820050205, 1998.

Hagemann, S. and Dümenil Gates, L.: Validation of the hydrological cycle of ECMWF and NCEP reanalyses using the MPI hydrological discharge model, Journal of Geophysical Research: Atmospheres, 106, 1503–1510, https://doi.org/10.1029/2000JD900568, 2001.

Hagemann, S. and Stacke, T.: Complementing ERA5 and E-OBS with high-resolution river discharge over Europe, Oceanologia, https://doi.org/10.1016/J.OCEANO.2022.07.003, 2022.

Hagemann, S., Stacke, T., and Ho-Hagemann, H. T.: High Resolution Discharge Simulations Over Europe and the Baltic Sea Catchment, Frontiers in Earth Science, 8, 12, https://doi.org/10.3389/FEART.2020.00012/BIBTEX, 2020.

Hale, R. L., Grimm, N. B., Vörösmarty, C. J., and Fekete, B.: Nitrogen and phosphorus fluxes from watersheds of the northeast U.S. from 1930 to 2000: Role of anthropogenic nutrient inputs, infrastructure, and runoff, Global Biogeochemical Cycles, 29, 341–356, https://doi.org/10.1002/2014GB004909, 2015.

Hamid, H. and Li, L.: Role of wastewater treatment plant (WWTP) in environmental cycling of poly- and perfluoroalkyl (PFAS) compounds, Ecocycles, 2, https://doi.org/10.19040/ecocycles.v2i2.62, 2016.

Hansson, K., Cousins, A. P., Norström, K., Graae, L., and Stenmarck, Å.: Sammanställning av befintlig kunskap om föroreningskällor till PFAS-ämnen i svensk miljö, p. NR C182, www.ivl.se, 2016.

Hepburn, E., Madden, C., Szabo, D., Coggan, T. L., Clarke, B., and Currell, M.: Contamination of groundwater with per- and polyfluoroalkyl substances (PFAS) from legacy landfills in an urban re-development precinct, Environmental Pollution, 248, 101–113, https://doi.org/10.1016/J.ENVPOL.2019.02.018, 2019.

Heydebreck, F., Tang, J., Xie, Z., and Ebinghaus, R.: Alternative and Legacy Perfluoroalkyl Substances: Differences between European and Chinese River/Estuary Systems, Environmental Science and Technology, 49, 8386–8395, https://doi.org/10.1021/acs.est.5b01648, 2015.

Holland, R., Khan, M. A. H., Chhantyal-Pun, R., Orr-Ewing, A. J., Percival, C. J., Taatjes, C. A., and Shallcross, D. E.: Investigating the atmospheric sources and sinks of perfluorooctanoic acid using a global chemistry transport model, Atmosphere, 11, 1–13, https://doi.org/10.3390/ATMOS11040407, 2020.

ICAO: Doc 9137 - Airport Services Manual Part 1, 2014.

ICPDR: Joint Danube Survey 3: Overview Map, p. 1, 2003.

Jin, Y. H., Liu, W., Sato, I., Nakayama, S. F., Sasaki, K., Saito, N., and Tsuda, S.: PFOS and PFOA in environmental and tap water in China, Chemosphere, 77, 605–611, https://doi.org/10.1016/J.CHEMOSPHERE.2009.08.058, 2009.

Joerss, H. K.: Legacy and Emerging Per- and Polyfluoroalkyl Substances in the Aquatic Environment – Sources , Sinks and Long-Range Transport to the Arctic, 2020.

Kannan, K., Corsolini, S., Falandysz, J., Oehme, G., Focardi, S., and Giesy, J. P.: Perfluorooctanesulfonate and related fluorinated hydrocarbons in marine mammals, fishes, and birds from coasts of the Baltic and the Mediterranean Seas, Environmental Science and Technology, 36, 3210–3216, https://doi.org/10.1021/ES020519Q/SUPPL_FILE/ES020519Q_S.PDF, 2002.

https://doi.org/10.5194/essd-2024-236
Preprint. Discussion started: 30 October 2024

Kirk, M., Smurthwaite, K., Bräunig, J., Trevenar, S., Lucas, R., Lal, A., Korda, R., Clements, A., Mueller, J., and Armstrong, B. P.: The PFAS health study systematic literature review, Canberra: The Australian National University, http://nceph.anu.edu.au/, 2018.

Kuenen, J., Dellaert, S., Visschedijk, A., Jalkanen, J. P., Super, I., and Denier Van Der Gon, H.: CAMS-REG-v4: a state-of-the-art high-resolution European emission inventory for air quality modelling, Earth System Science Data, 14, 491–515, https://doi.org/10.5194/ESSD-14-491-2022, 2022.

Kummu, M., Taka, M., and Guillaume, J. H.: Gridded global datasets for Gross Domestic Product and Human Development Index over 1990-2015, Scientific Data, 5, 1–16, https://doi.org/10.1038/sdata.2018.4, 2018.

Lang, J. R., Allred, B. M. K., Field, J. A., Levis, J. W., and Barlaz, M. A.: National Estimate of Per- and Polyfluoroalkyl Substance (PFAS) Release to U.S. Municipal Landfill Leachate, Environmental Science and Technology, 51, 2197–2205, https://doi.org/10.1021/ACS.EST.6B05005/SUPPL_FILE/ES6B05005_SI_002.XLSX, 2017.

Langenbach, B., Wilson, M., Zhang, T., Kim, U.-J., and Pilar Martinez Moral, M.: Per- and Polyfluoroalkyl Substances (PFAS): Significance and Considerations within the Regulatory Framework of the USA, International Journal of Environmental Research and Public Health 2021, Vol. 18, Page 11142, 18, 11 142, https://doi.org/10.3390/IJERPH182111142, 2021.

Lim, T. C., Wang, B., Huang, J., Deng, S., and Yu, G.: Emission inventory for PFOS in China: Review of past methodologies and suggestions, TheScientificWorldJournal, 11, 1963–1980, https://doi.org/10.1100/2011/868156, 2011.

Linderoth, M., Hellström, A., Lilja, K., Nordin, A., Hedman, J., and Klingspor, K.: Högfluorerade ämnen (PFAS) och bekämpningsmedel -, ISBN 9789162067090, 2016.

Lindim, C., Cousins, I. T., and Vangils, J.: Estimating emissions of PFOS and PFOA to the Danube River catchment and evaluating them using a catchment-scale chemical transport and fate model, Environmental Pollution, 207, 97–106, https://doi.org/10.1016/j.envpol.2015.08.050, 2015a.

Lindim, C., Cousins, I. T., and Vangils, J.: Estimating emissions of PFOS and PFOA to the Danube River catchment and evaluating them using a catchment-scale chemical transport and fate model, Environmental Pollution, 207, 97–106, https://doi.org/10.1016/J.ENVPOL.2015.08.050, 2015b.

Liška, I., Wagner, F., Sengl, M., Deutsch, K., and Slobodník, J.: Joint Danube Survey 3: A Comprehensive Analysis of Danube Water Quality, ISBN 9783200037953, http://www.danubesurvey.org/results, 2015.

Loos, R., Gawlik, B. M., Locoro, G., Rimaviciute, E., Contini, S., and Bidoglio, G.: EU-wide survey of polar organic persistent pollutants in European river waters, Environmental Pollution, 157, 561–568, https://doi.org/10.1016/j.envpol.2008.09.020, 2009.

Martin, J. W., Mabury, S. A., Solomon, K. R., and Muir, D. C.: Dietary accumulation of perfluorinated acids in juvenile rainbow trout (Oncorhynchus mykiss), Environmental Toxicology and Chemistry, 22, 189–195, https://doi.org/10.1002/ETC.5620220125, 2003.

Matthias, V., Arndt, J. A., Aulinger, A., Bieser, J., Denier van der Gon, H., Kranenburg, R., Kuenen, J., Neumann, D., Pouliot, G., and Quante, M.: Modeling emissions for three-dimensional atmospheric chemistry transport models, https://doi.org/10.1080/10962247.2018.1424057, 68, 763–800, https://doi.org/10.1080/10962247.2018.1424057, 2018.

Mclachlan, M. S., Holmstrom, K. E., Reth, M., and Berger, U.: Riverine discharge of perfluorinated carboxylates from the European continent, Environmental Science and Technology, 41, 7260–7265, https://doi.org/10.1021/es071471p, 2007.

Munoz, G., Liu, J., Vo Duy, S., and Sauvé, S.: Analysis of F-53B, Gen-X, ADONA, and emerging fluoroalkylether substances in environmental and biomonitoring samples: A review, Trends in Environmental Analytical Chemistry, 23, e00066, https://doi.org/10.1016/J.TEAC.2019.E00066, 2019.

Nace, R.: Statistical classification of economic activities in the European Community.

https://doi.org/10.5194/essd-2024-236
Preprint. Discussion started: 30 October 2024

OECD: Results of Survey on Production and Use of PFOS, PFAS, and PFOA, Related Substances and Products/Mixtures Containing These Substances, Proceedings of the ENVIRONMENT DIRECTORATE The Joint Meeting of the Chemicals Committee and Working Party on Chemicals, Pesticides and Biotechnology, ENV/JM/ MONO(2006, p. 36, http://www.oecd.org/officialdocuments/publicdisplaydocumentpdf/?doclanguage=en&cote=env/jm/mono(2005)1, 2004.

OECD: Substance Information Data-Sheet (SIDS), Assessment Profile for Perfluorooctanoic Acid (PFOA), Ammonium Perfluorooctanoate (APFO), SIDS Initial Assessment Meeting, p. 5, https://hpvchemicals.oecd.org/UI/handler.axd?id=1f391916-96ba-46f6-a7ce-c96712da3b7e, 2006.

OECD: PFCs: Outcome of the 2009 Survey. Survey on the production, use and release of PFOS, PFAS, PFOA PFCA, their related substances and products/mixtures containing these substances, p. 61, http://www.oecd.org/officialdocuments/publicdisplaydocumentpdf/?cote=env/jm/mono(2011)1&doclanguage=en, 2011.

OECD Environment Directorate: Toward a New Comprehensive Global Database of Per- and Polyfluoroalkyl Substances (PFASs): Summary Report on Updating the OECD 2007 List of Per- and Polyfluoroalkyl Substances (PFASs), Tech. rep., 2018.

Paustenbach, D. J., Panko, J. M., Scott, P. K., and Unice, K. M.: A methodology for estimating human exposure to perfluorooctanoic acid (PFOA): A retrospective exposure assessment of a community (1951-2003), Journal of Toxicology and Environmental Health - Part A: Current Issues, 70, 28–57, https://doi.org/10.1080/15287390600748815, 2007a.

Paustenbach, D. J., Panko, J. M., Scott, P. K., and Unice, K. M.: A methodology for estimating human exposure to perfluorooctanoic acid (PFOA): A retrospective exposure assessment of a community (1951-2003), Journal of Toxicology and Environmental Health - Part A: Current Issues, 70, 28–57, https://doi.org/10.1080/15287390600748815, 2007b.

Pétré, M. A., Salk, K. R., Stapleton, H. M., Ferguson, P. L., Tait, G., Obenour, D. R., Knappe, D. R., and Genereux, D. P.: Per- and polyfluoroalkyl substances (PFAS) in river discharge: Modeling loads upstream and downstream of a PFAS manufacturing plant in the Cape Fear watershed, North Carolina, Science of The Total Environment, 831, 154 763, https://doi.org/10.1016/J.SCITOTENV.2022.154763, 2022.

Pickard, H. M., Ruyle, B. J., Thackray, C. P., Chovancova, A., Dassuncao, C., Becanova, J., Vojta, S., Lohmann, R., and Sunderland, E. M.: PFAS and Precursor Bioaccumulation in Freshwater Recreational Fish: Implications for Fish Advisories, Environmental Science and Technology, 56, 15 573–15 583, https://doi.org/10.1021/acs.est.2c03734, 2022.

Pistocchi, A. and Loos, R.: A map of European emissions and concentrations of PFOS and PFOA, Environmental Science and Technology, 43, 9237–9244, https://doi.org/10.1021/es901246d, 2009.

Post, G. B., Cohn, P. D., and Cooper, K. R.: Perfluorooctanoic acid (PFOA), an emerging drinking water contaminant: A critical review of recent literature, Environmental Research, 116, 93–117, https://doi.org/10.1016/j.envres.2012.03.007, 2012.

Prevedouros, K., Cousins, I. T., Buck, R. C., and Korzeniowski, S. H.: Sources, fate and transport of perfluorocarboxylates, https://doi.org/10.1021/es0512475, 2006.

Scheringer, M., Trier, X., Cousins, I. T., de Voogt, P., Fletcher, T., Wang, Z., and Webster, T. F.: Helsingør Statement on poly- and perfluorinated alkyl substances (PFASs), Chemosphere, 114, 337–339, https://doi.org/10.1016/J.CHEMOSPHERE.2014.05.044, 2014.

Shin, H. M., Vieira, V. M., Ryan, P. B., Detwiler, R., Sanders, B., Steenland, K., and Bartell, S. M.: Environmental fate and transport modeling for perfluorooctanoic acid emitted from the Washington works facility in West Virginia, Environmental Science and Technology, 45, 1435–1442, https://doi.org/10.1021/ES102769T/SUPPL_FILE/ES102769T_SI_001.PDF, 2011.

Simon, P.: POPE model and data v2.0, https://doi.org/10.5281/zenodo.12783504, 2024.

Soerensen, A. and Faxneld, S.: Per- and polyfluoroalkyl substances (PFAS) within the Swedish Monitoring Program for Contaminants in Marine Biota, 6, 1–56, 2023.

https://doi.org/10.5194/essd-2024-236
Preprint. Discussion started: 30 October 2024

Stemmler, I. and Lammel, G.: Pathways of PFOA to the Arctic: Variabilities and contributions of oceanic currents and atmospheric transport and chemistry sources, Atmospheric Chemistry and Physics, 10, 9965–9980, https://doi.org/10.5194/ACP-10-9965-2010, 2010.

Sun, M., Arevalo, E., Strynar, M., Lindstrom, A., Richardson, M., Kearns, B., Pickett, A., Smith, C., and Knappe, D. R.: Legacy and Emerging Perfluoroalkyl Substances Are Important Drinking Water Contaminants in the Cape Fear River Watershed of North Carolina, Environmental Science and Technology Letters, 3, 415–419, https://doi.org/10.1021/ACS.ESTLETT.6B00398/SUPPL_FILE/EZ6B00398_SI_001.PDF, 2016.

Thackray, C. P. and Selin, N. E.: Uncertainty and variability in atmospheric formation of PFCAs from fluorotelomer precursors, Atmospheric Chemistry and Physics, 17, 4585–4597, https://doi.org/10.5194/acp-17-4585-2017, 2017.

UNEP: Stockholm Convention on Persistent Organic Pollutants (POPs), 2020.

Vierke, L., Staude, C., Biegel-Engler, A., Drost, W., and Schulte, C.: Perfluorooctanoic acid (PFOA)-main concerns and regulatory developments in Europe from an environmental point of view, Environmental Sciences Europe, 24, 1–11, https://doi.org/10.1186/2190-4715-24-16, 2012.

Wang, Z., Cousins, I. T., Scheringer, M., and Hungerbühler, K.: Fluorinated alternatives to long-chain perfluoroalkyl carboxylic acids (PFCAs), perfluoroalkane sulfonic acids (PFSAs) and their potential precursors, Environment International, 60, 242–248, https://doi.org/10.1016/J.ENVINT.2013.08.021, 2013.

Wang, Z., Cousins, I. T., Scheringer, M., Buck, R. C., and Hungerbühler, K.: Global emission inventories for C4-C14 perfluoroalkyl carboxylic acid (PFCA) homologues from 1951 to 2030, Part I: Production and emissions from quantifiable sources, https://doi.org/10.1016/j.envint.2014.04.013, 2014a.

Wang, Z., Cousins, I. T., Scheringer, M., Buck, R. C., and Hungerbühler, K.: Global emission inventories for C4-C14 perfluoroalkyl carboxylic acid (PFCA) homologues from 1951 to 2030, part II: The remaining pieces of the puzzle, Environment International, 69, 166–176, https://doi.org/10.1016/j.envint.2014.04.006, 2014b.

Wang, Z., Boucher, J. M., Scheringer, M., Cousins, I. T., and Hungerbühler, K.: Toward a Comprehensive Global Emission Inventory of C4-C10 Perfluoroalkanesulfonic Acids (PFSAs) and Related Precursors: Focus on the Life Cycle of C8-Based Products and Ongoing Industrial Transition, Environmental Science and Technology, 51, 4482–4493, https://doi.org/10.1021/acs.est.6b06191, 2017.

Will, R.; Kälin, T. K. A.: Fluoropolymers. In CEH Marketing Research Report, SRI International: Menlo Park, CA, 2005.

Xu, B., Liu, S., Zhou, J. L., Zheng, C., Weifeng, J., Chen, B., Zhang, T., and Qiu, W.: PFAS and their substitutes in groundwater: Occurrence, transformation and remediation, Journal of Hazardous Materials, 412, 125 159, https://doi.org/10.1016/j.jhazmat.2021.125159, 2021.

Yarwood, G., Kemball-Cook, S., Keinath, M., Waterland, R. L., Korzeniowski, S. H., Buck, R. C., Russell, M. H., and Washburn, S. T.: High-resolution atmospheric modeling of fluorotelomer alcohols and perfluorocarboxylic acids in the North American troposphere, Environmental Science and Technology, 41, 5756–5762, https://doi.org/10.1021/ES0708971, 2007.

Zarębska, M., Bajkacz, S., and Hordyjewicz-Baran, Z.: Assessment of legacy and emerging PFAS in the Oder River: Occurrence, distribution, and sources, Environmental research, 251, https://doi.org/10.1016/J.ENVRES.2024.118608, 2024.